Applied Remote Sensing for Improved Transboundary Water Resource Management in the Lower Mekong River Basin

John Bolten (NASA GSFC)

Motivation

Figure 8. Population exposed to sea-level rise, storm surge and subsidence by country (for scenario FAC). Total estimated exposure is 147 million people.

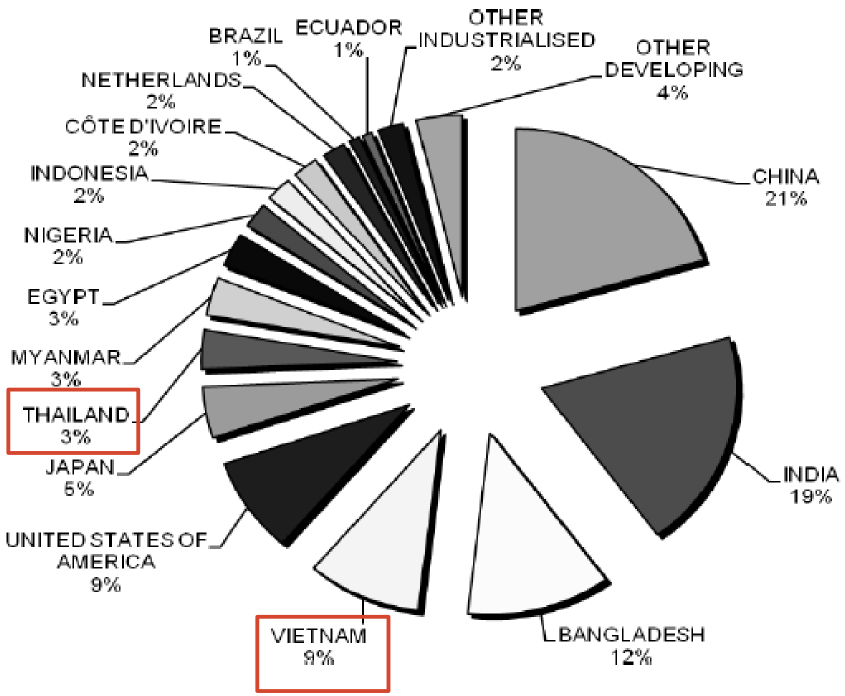

Flooding in the Mekong

- Floods are among the **most common and damaging** natural disasters
- Coastal and low-lying regions are particularly susceptible*
- Climate change effects are likely to increase flood risks

* Reference: Nicholls, R. J. et al. Ranking Port Cities with High Exposure and Vulnerability to Climate Extremes. (Organisation for Economic Co-operation and Development, 2008)

Motivation

Việt Nam News
THE NATIONAL ENGLISH LANGUAGE DAILY

Early floods threaten Mekong rice fields

August 5, 2017

REUTERS

Typhoon Damrey kills 106 in Vietnam, reservoirs brimming before APEC

Mai Nguyen November 8, 2017

Flooding in the Mekong

- Floods are among the **most common and damaging** natural disasters
- Coastal and low-lying regions are particularly susceptible*
- Climate change effects are likely to increase flood risks

It is critical to understand the **impacts** of flood events to improve disaster response and flood mitigation at local and regional levels

* Reference: Nicholls, R. J. et al. Ranking Port Cities with High Exposure and Vulnerability to Climate Extremes. (Organisation for Economic Co-operation and Development, 2008)

The Water Landscape

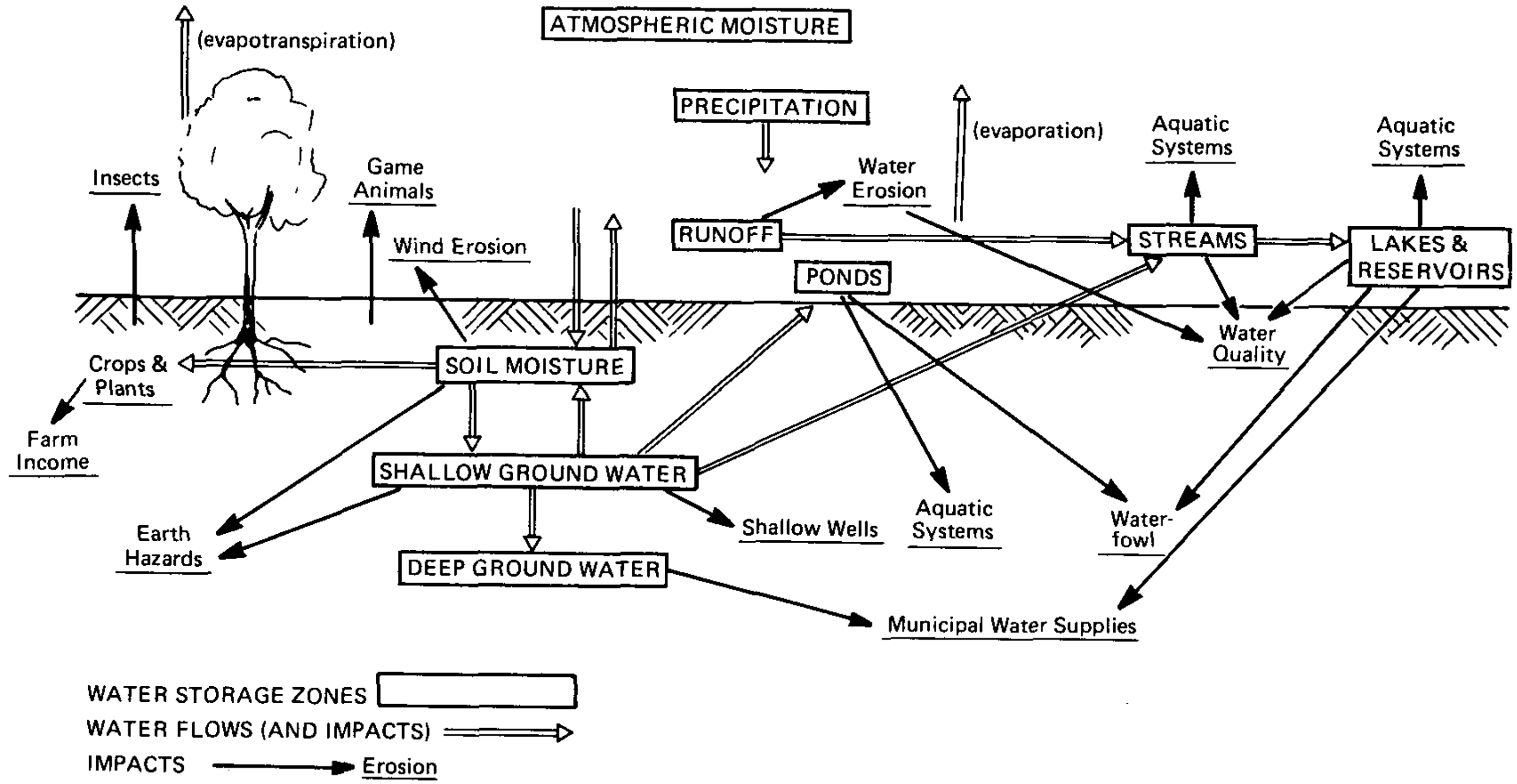

Image Credit: Chagnon, 1989

- How can we reduce our uncertainty propagation of hydroclimatic extremes?
- For example, will a meteorological drought lead to a hydrological or agricultural drought?
  - How? When? Where?
- How do phases in P-E relate to soil moisture, surface drainage, base flow, groundwater storage, river discharge, and vegetation productivity?

Closing the Terrestrial Water Budget Using Remote Sensing

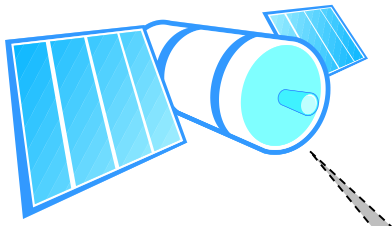

Rn: Radiation
Shortwave: GOES
Longwave: AIRS/AMSU

H, G: Surface Temperature
AIRS, AVHRR, MODIS

Clouds: GOES
Water Vapor (LE): AIRS/AMSU

The land surface water and energy budgets are linked via evapotranspiration

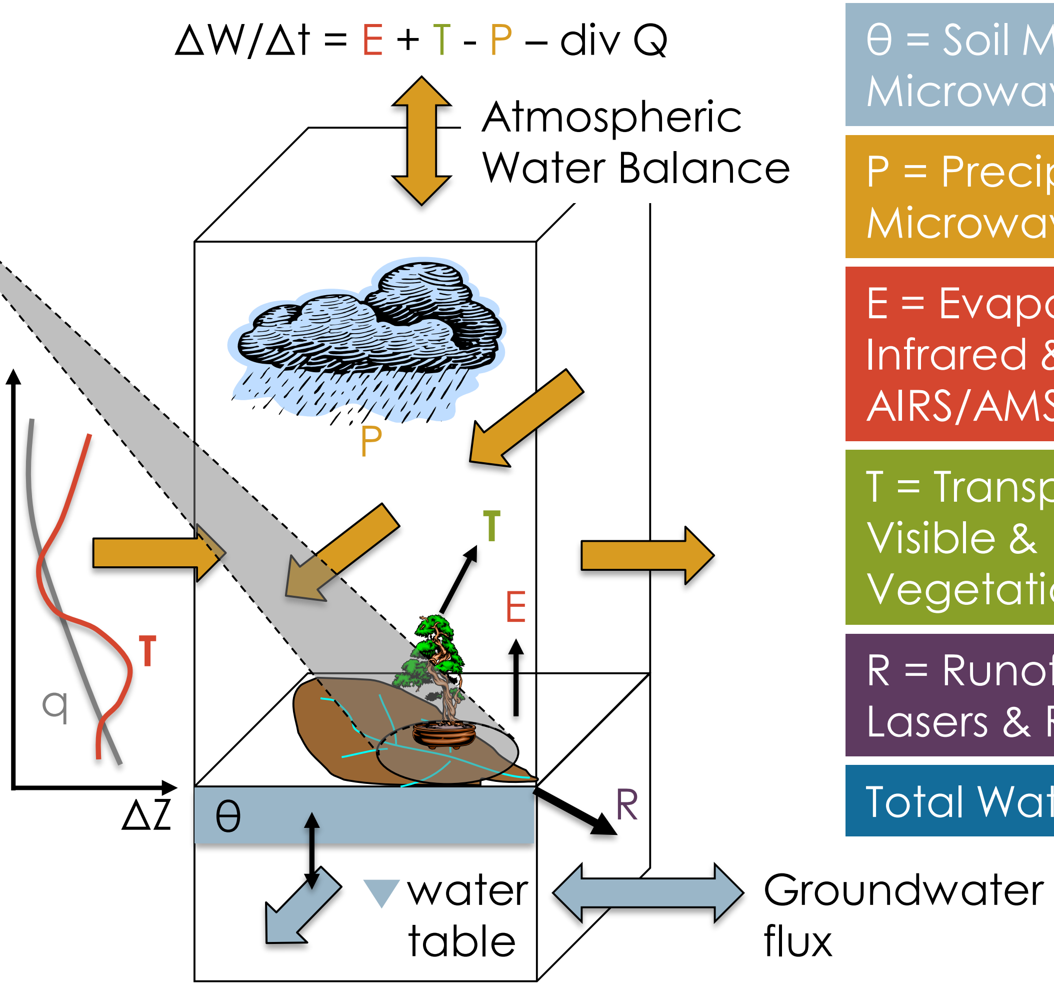

θ = Soil Moisture
Microwave Radiation: AMSR, SMOS, SMAP

P = Precipitation
Microwave Radiation: SSM/I, TRMM, GPM

E = Evaporation/Surface Humidity
Infrared & Microwave Radiation: AIRS/AMSU

T = Transpiration/NDVI
Visible & NIR: MODIS, AVHRR, GLI, VCL
Vegetation: NDVI, AVHRR, MODIS, Landsat

R = Runoff/River Level
Lasers & Radar: TOPEX, Radarsat, SWOT*

Total Water/Groundwater: GRACE

Energy Balance
$Rn + H + LE + G = 0$

Water Balance
$\Delta Z\ \Delta\theta/\Delta t = P - E - T - R$

2018. "Global Hydrological Cycles and Water Resources." *National Academies of Sciences, Engineering, and Medicine. 2018. Thriving on Our Changing Planet: A Decadal Strategy for Earth Observation from Space*, Washington, DC: The National Academies Press [10.17226/24938]

Satellites, Sensors, and Timelines

Atmosphere
Terra/Aqua (AIRS): water vapor profile, clouds, air temp profile, surface temperature, 12.5 km (2000 - present)

Total Water
GRACE (2002-2017)
GRACE-FO: 100 km (2018-present)

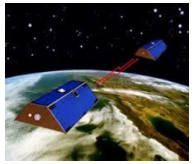

Rainfall
TRMM: 25 km, 3-hr (1998-2015)
GPM: 10 km, 30 min (2014 – present)

Soil Moisture
Aqua (AMSR-E): c-band radar (2002-2015);
(AMSR): 25 km (2002-2011)
SMAP: L-band radar (2015); 36 km (2015-present)
SMOS: 25 km (2009-present)

Wetness Rainfall
Nimbus-7 (SMMR): C-band 150 km (1978 – 1987)
DMSP-F8-13 (SSM/I) and DMSP-F15-18 (SSMIS): wetness, rainfall, clouds 12-50 km (1987–present)

Vegetation
NOAA-15 (AVHRR): NDVI, surface temperature 4 km (1980 - present)
Terra/Aqua (MODIS): NDVI, surface temperature 1 km (2000 - present)

Surface Temperature
Landsat: Vegetation, Land-Use Land Cover 30 m

1980 1990 2000 2010 2020

Objective

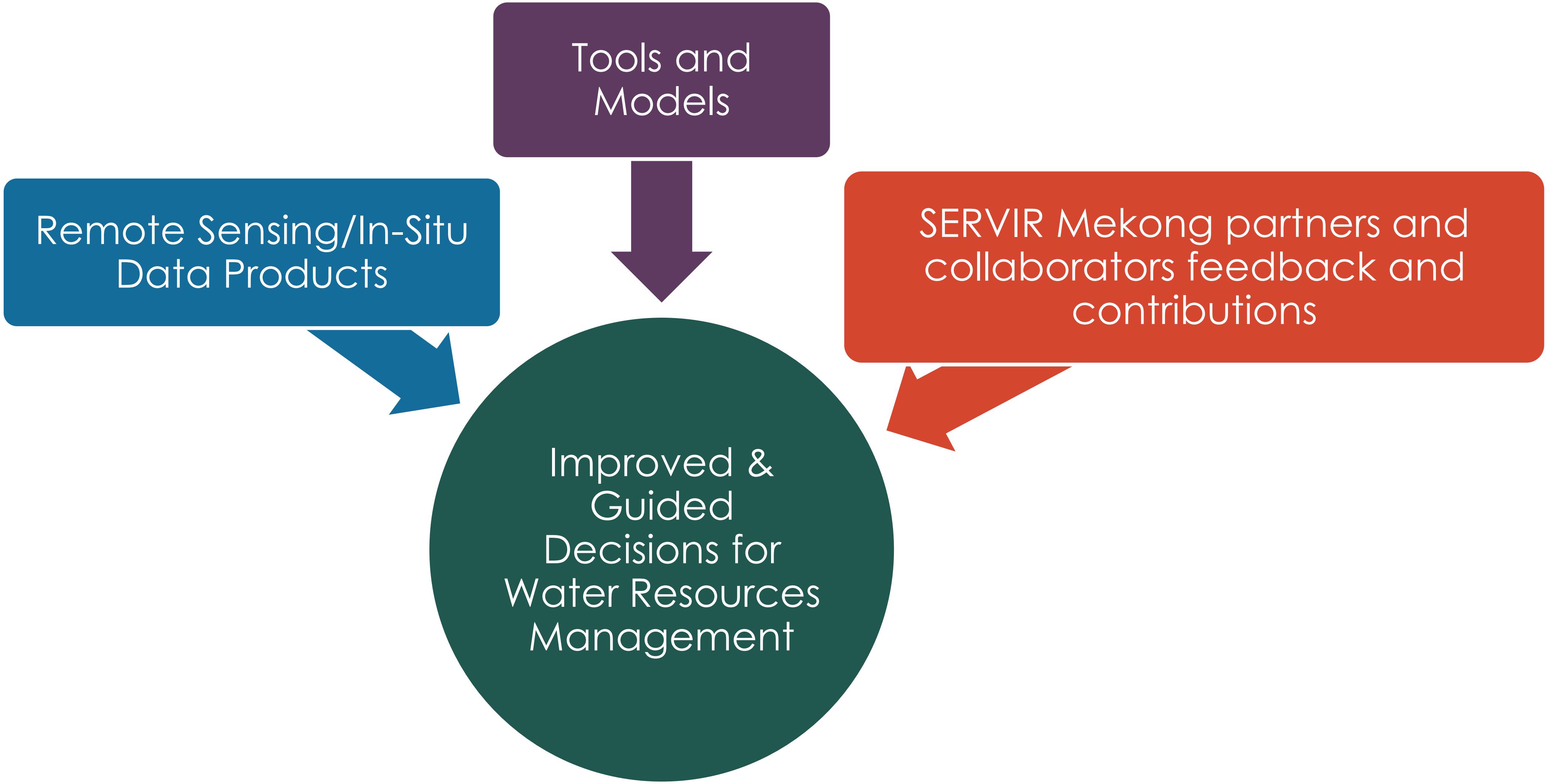
Tools and Models
Remote Sensing/In-Situ Data Products
SERVIR Mekong partners and collaborators feedback and contributions
Improved & Guided Decisions for Water Resources Management

Hydrologic Decision Support System for the Lower Mekong River Basin

- The LMRB (drainage area of ~ 495,000 km2) SWAT Model setup closely follows MRC sub-basin configuration [Rossi et al., 2009]
- A digital elevation model (DEM) with 1 arc-sec grid resolution, ASTER was adopted
- Harmonized World Soil Database [FAO et al., 2012], version 1.2 was implemented
- MODIS, NDVI, Landsat TM, and ETM+ data products were used to obtain lower Mekong Basin LULC map

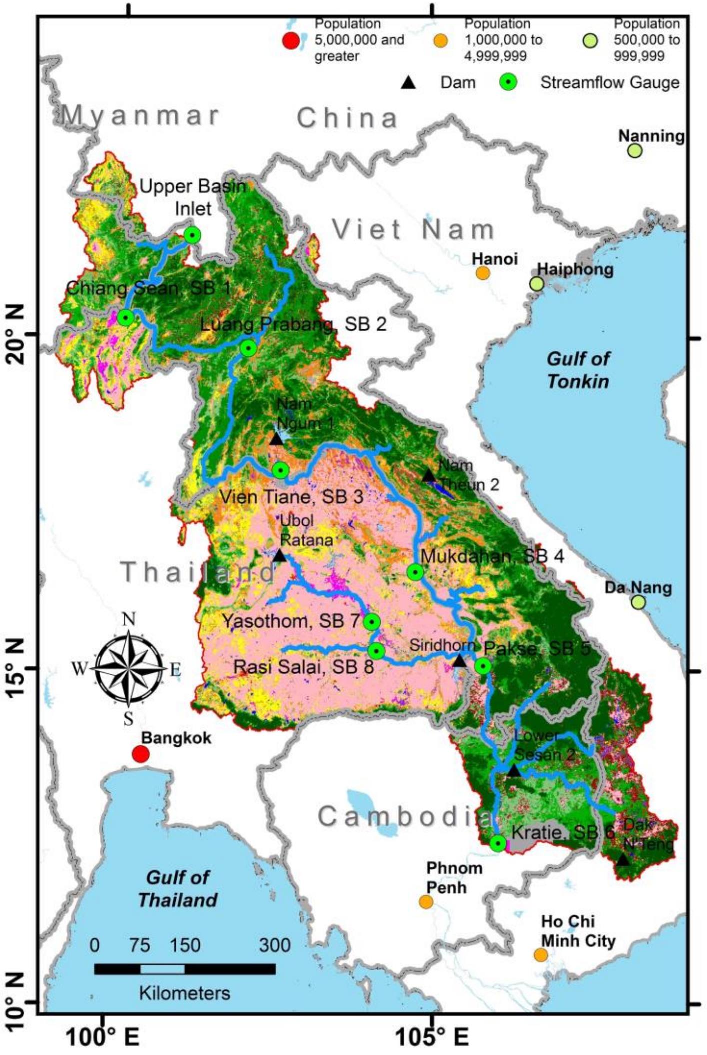

Discharge data obtained from the Mekong River Commission (MRC, www.mrcmekong.org)
Updated discharge data were interpolated from recent observed level data obtained from the Asian Preparedness Disaster Center (ADPC, www.adpc.net)

Rossi, et. al., 2009. Hydrologic evaluation of the lower Mekong River Basin with the soil and water assessment tool model. IAEJ 18, 1-13, http://114.255.9.31/iaej/EN/Y2009/V18/I01-02/1

SWAT: Soil and Water Assessment Tool

https://swat.tamu.edu/

- SWAT is a conceptual watershed-scale hydrological model designed to address challenges related to water management, sediment, climate change, land use change, and agricultural chemical yield
- The SWAT applications range from the field scale to the watershed scale to the continental scale
- The SWAT model components are hydrology, weather, sedimentation, soil temperature, crop growth, nutrients, pesticides, and agricultural management

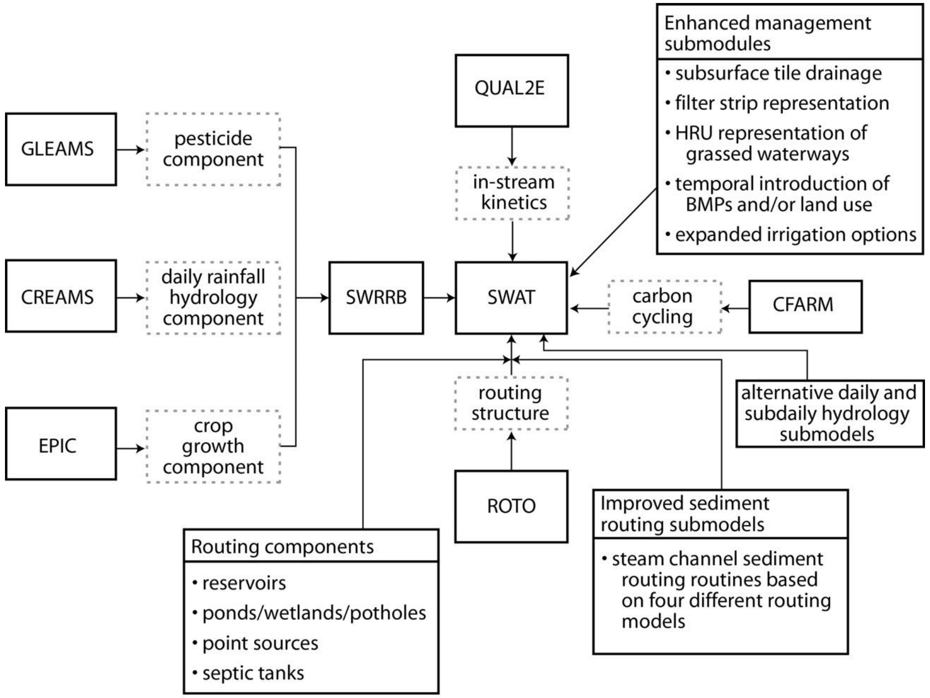

Schematic of SWAT development history and model adaptations (adapted from Grassman*)

* Reference: Gassman, P.W., Reyes, M.R., Green, C.H., Arnold, J.G., 2007. The soil and water assessment tool: Historical development, applications, and future research directions. T ASABE 50, 1211-1250, https://doi.org/10.13031/2013.23637

LMB LULC Types That Can Affect Hydrology and SWAT Hydrologic Modeling Results

- Agriculture LULC Types
  - Rain fed vs. irrigated rice (single vs. double-cropped)
  - Other annual crops (e.g., row crops, sugar cane, cassava)
  - Shifting vs. permanent field crop cultivation
- Forest LULC Types
  - Mainly broadleaved with different levels of deciduousness
  - Gradient of nearly pristine to highly disturbed forests
  - Bamboo habitats
  - Industrial forest plantations (e.g., rubber)
- Other LULC Classes
  - water, barren, urban

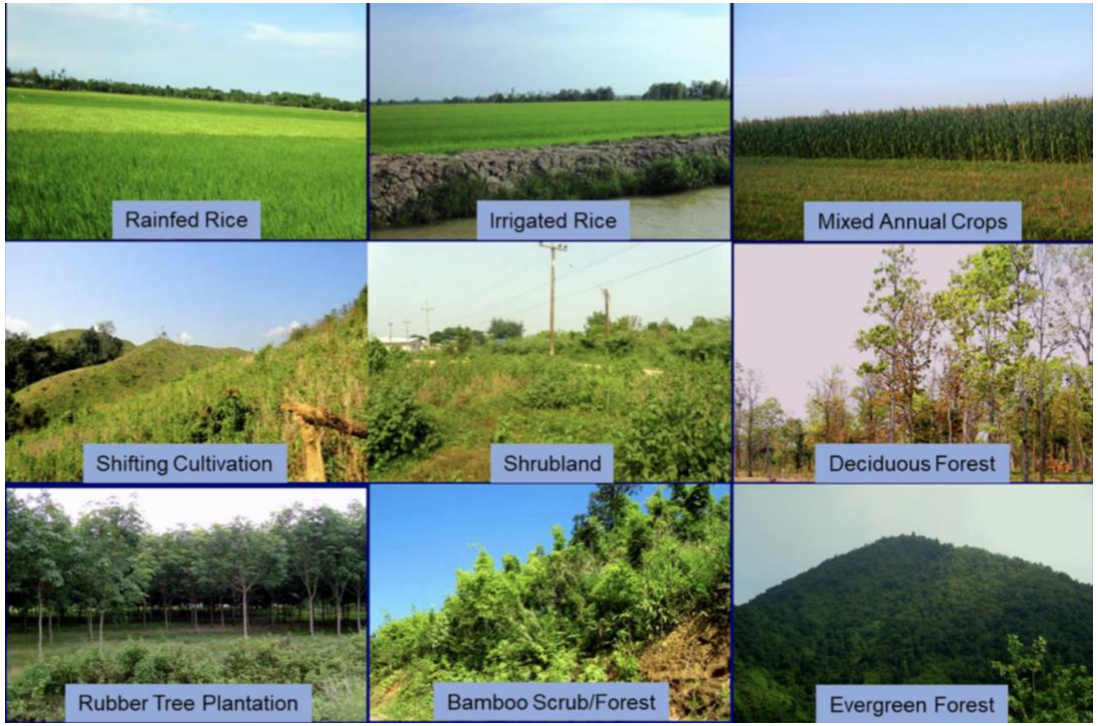

Photos of Lower Mekong Basin LULC types were acquired from the Mekong River Commission

Spruce, J., J. Bolten, R. Srinivasan, and V. Lakshmi. 2018. "Developing Land Use Land Cover Maps for the Lower Mekong Basin to Aid Hydrologic Modeling and Basin Planning." Remote Sensing, 10 (12): 1910 [10.3390/rs10121910]

Workflow for Deriving LULC Maps

MOD09 8-day Reflectance

MOD35 Clouds, Shadows

MOD03 Geolocation

Process MOD09/MYD09 Reflectance into 32-Day NDVI Data with Time Series Product Tool (TSPT)

- Remove clouds and shadows
- Reduce residual noise
- Constrain viewing geometry
- Fuse Terra/Aqua products
- Interpolate data voids
- Savitzky-Golay filtering
- Re-aggregate as 32-day composites
- 12 products per year

Landsat – TOA Reflectance Mosaic

LULC Classification

- Unsupervised Classification of 2010 MODIS NDVI data
- Unsupervised classification of finer scaled cover types from Landsat data
- LULC maps integrated with ERDAS Imagine software
- LULC maps assessed with MRC, Bing or Google aerial or satellite imagery, MODIS NDVI profiles, and Landsat data

- Landsat data from circa 2011 Landsat dry season mosaic
- 2010 MODIS 32-day NDVIs from dry season used for forest mapping
- All 12 dates of 2010 MODIS 32-day NDVIs used to map agriculture

Spruce, J., J. Bolten, R. Srinivasan, and V. Lakshmi. 2018. "Developing Land Use Land Cover Maps for the Lower Mekong Basin to Aid Hydrologic Modeling and Basin Planning." Remote Sensing, 10 (12): 1910 [10.3390/rs10121910]

1997 to 2010 LULC Change Map of LMB - 9 LULC Classes Per Date

Color	No Change - LULC Class Description
	no change - barren
	no change - urban
	no change - annual crops
	no change - shifting cultivation
	no change - scrub/shrub
	no change - deciduous forest/scrub
	no change - evergreen forest
	no change - industrial forest plantation
	no change - wetlands

Color	Change - LULC Class Description
	change to barren in 2010
	change to urban in 2010
	change to annual crops in 2010
	change to shifting cultivation in 2010
	change to scrub/shrub in 2010
	change to deciduous forest/scrub in 2010
	change to evergreen forest in 2010
	change to industrial forest plantation in 2010
	change to wetlands in 2010

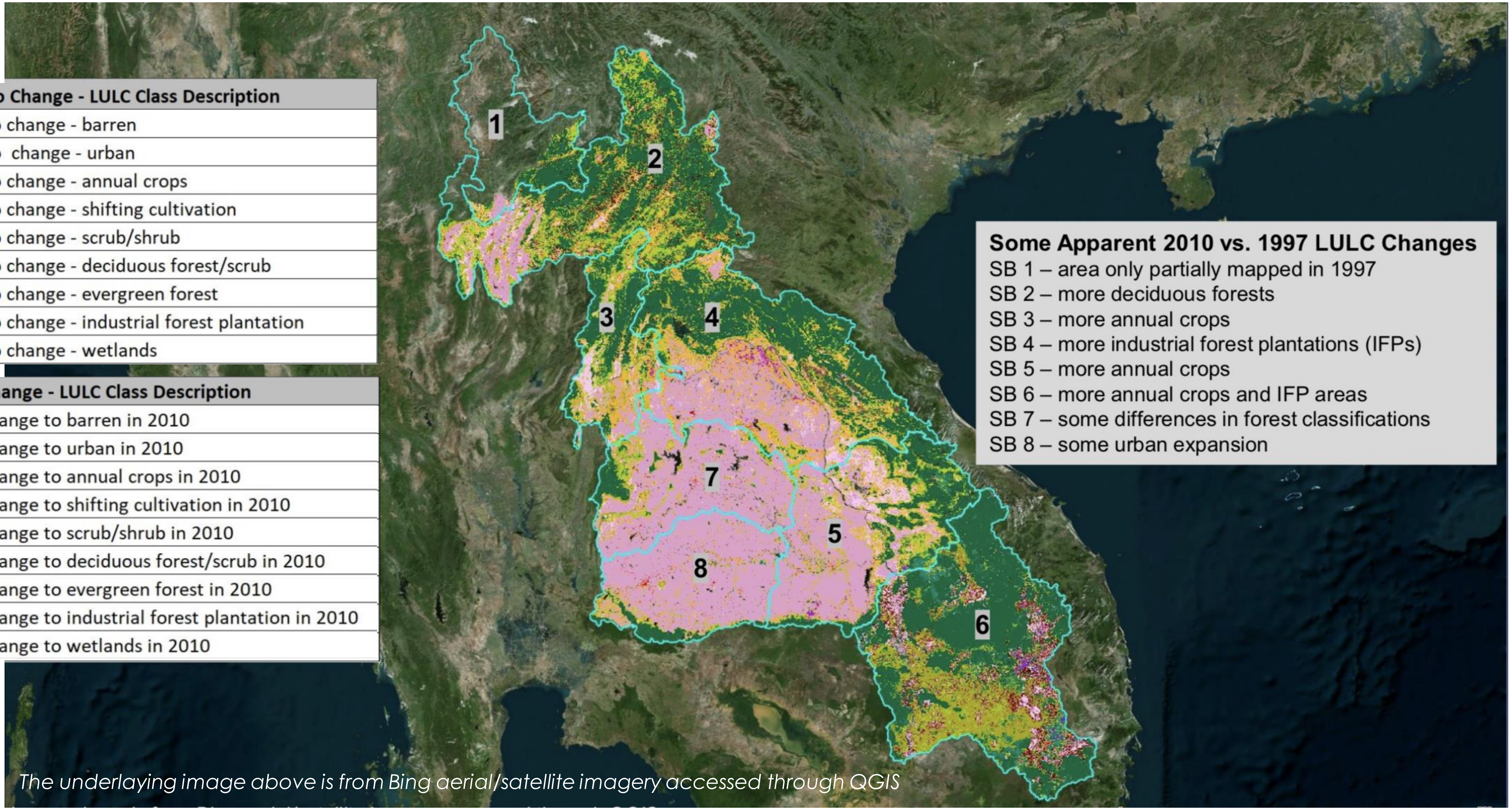

The underlaying image above is from Bing aerial/satellite imagery accessed through QGIS

Project 2010 LULC Map vs MRC Recoded 1997 LULC Map

(e.g., Subset of SB7)

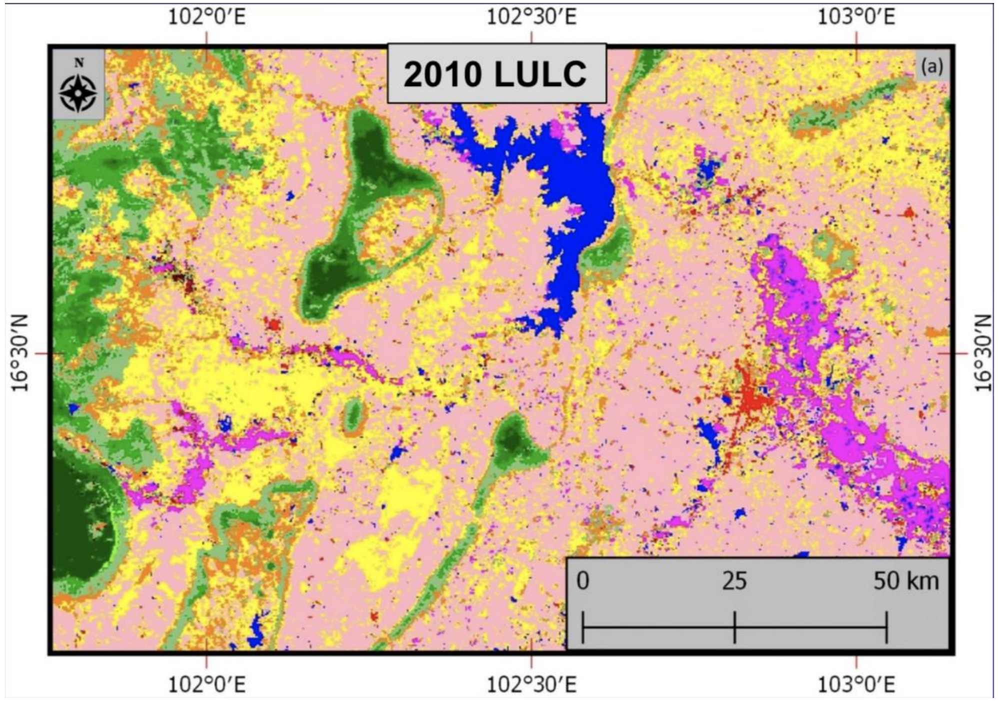

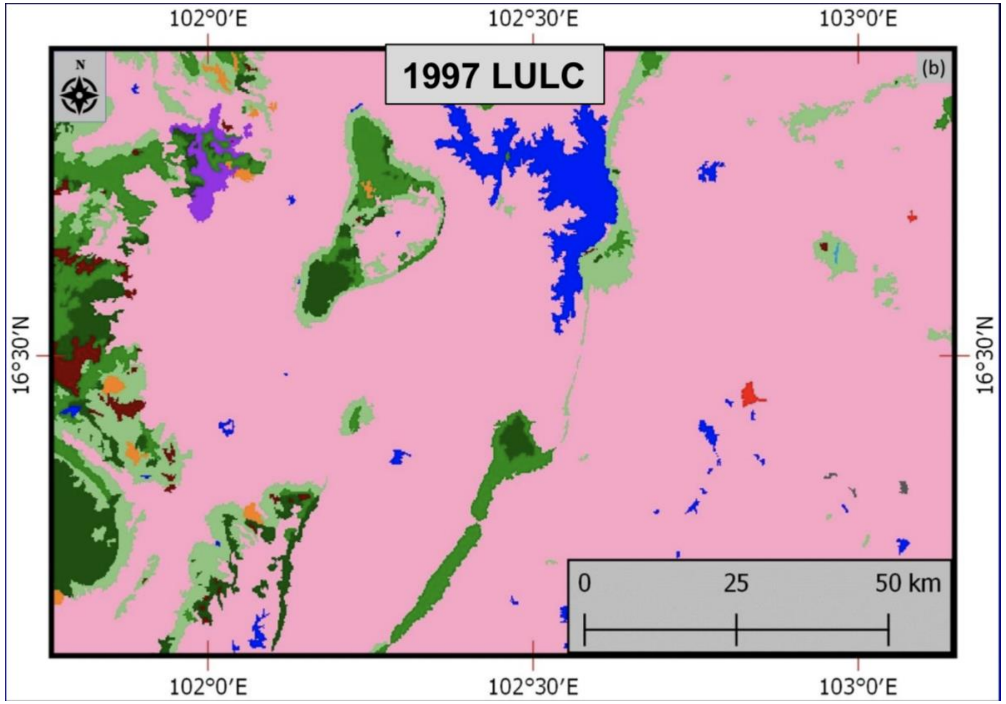

- The 2010 LULC map has multiple permanent agriculture types, while the 1997 LULC map only has one general permanent agriculture type
- The 2010 LULC map has a finer scaled minimum mapping unit vs. 1997 map (0.0625 km^2 vs. 0.5 km^2)
- The 2010 LULC map also shows more urban areas (bright red on maps above)

Images are from: Remote Sensing 2018, 10, 1910; doi: 10.3390/rs10121910

Summary: Key Points

- The project updated LULC maps for the Lower Mekong Basin that are being used in MRC SWAT models for SBs 1-8
  - 18 total LULC types were mapped for 2010 update of previous 1997 map
- Results of LULC accuracy assessments for SBs 4 and 7 both showed high overall agreements with reference data (80%+)
  - The 2010 LULC map included more permanent crop types than on the 1997 LULC map
  - Rice was mapped on the 2010 LULC map according to number of crops per year
  - MODIS NDVI data from dry season enabled mapping of basic deciduous and evergreen broadleaved forest types
  - Landsat multispectral data from dry season enabled mapping of scarce, finer, scaled LULC types (e.g., urban and open water areas)
- The project's LULC maps are being used in LMB SWAT models to aid water and disaster management
- For additional information, see paper in Remote Sensing 2018, 10, 1910: doi:10.3390/rs10121910

SWAT Calibration Parameters

Parameter	Description	Range
Precipitation	Correction factor	r__Precipitation(SB#s){}.pcp -0.6 0.01
	High Flows	
CN2	Initial SCS runoff curve number to moisture condition II	r__CN2.mgt -10 10
AWC	Available water capacity of the soil layer	r__SOL_AWC().sol -10 10
ESCO	Soil evaporation compensation factor	v__ESCO.bsn 0.5 0.9
	Base Flows	
GW_DELAY	Groundwater delay time	a__GW_DELAY.gw -30 60
REVAPMN	percolation to the deep aquifer to occur	a__REVAPMN.gw -750 750
GWQMN	Threshold depth of water in the shallow aquifer	a__GWQMN.gw -1000 1000
GW_REVAP	Groundwater "revap" coefficient	v__GW_REVAP.gw 0.02 0.1
RCHRG_DP	Deep aquifer percolation fraction	a__RCHRG_DP.gw -0.05 0.05
GWHT	Initial groundwater height	v__GWHT.gw 0.0 1.0

Mohammed, I. N., Bolten, J., Srinivasan, R., & Lakshmi, V. (2018). Improved Hydrological Decision Support System for the Lower Mekong River Basin Using Satellite-Based Earth Observations. Remote Sensing, 10(6), 885. http://dx.doi.org/10.3390/rs10060885

SWAT model with Remote Sensing Climate Input Data

- Minimum and maximum air temperature processed using GLDAS Noah Land Surface Model L4 3 hourly 0.25 x 0.25 degree V2.0

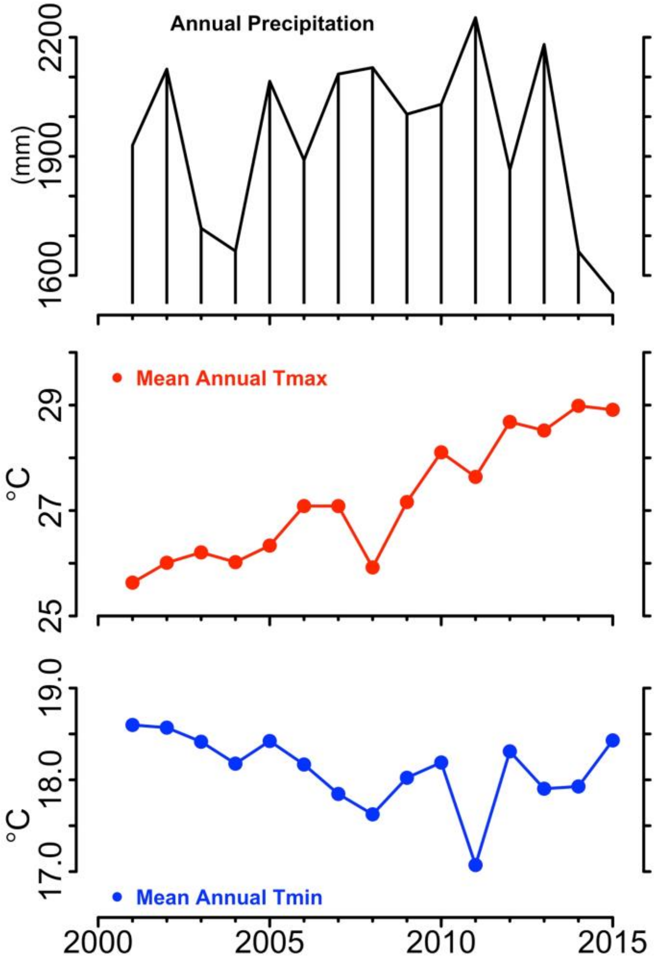

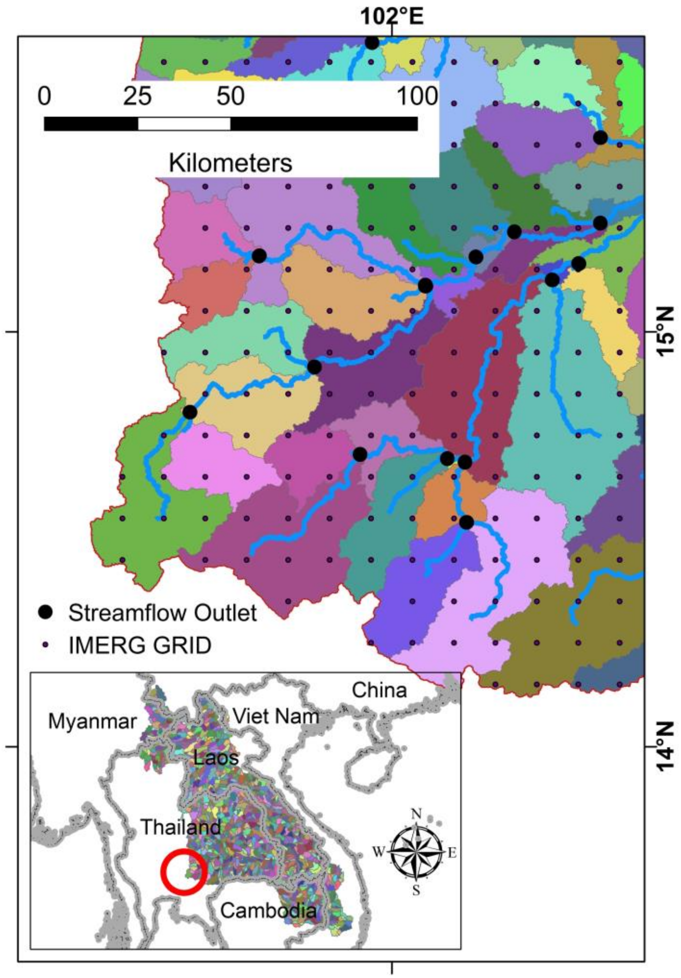

Mohammed, I. N., J. D. Bolten, R. Srinivasan, et al. 2018. "Ground and satellite based observation datasets for the Lower Mekong River Basin." Data in Brief, 21: 2020-2027 [10.1016/j.dib.2018.11.038]

SWAT Model Streamflow Calibration

- Sequential calibration from Upper Mekong inlet to Kratie, Cambodia

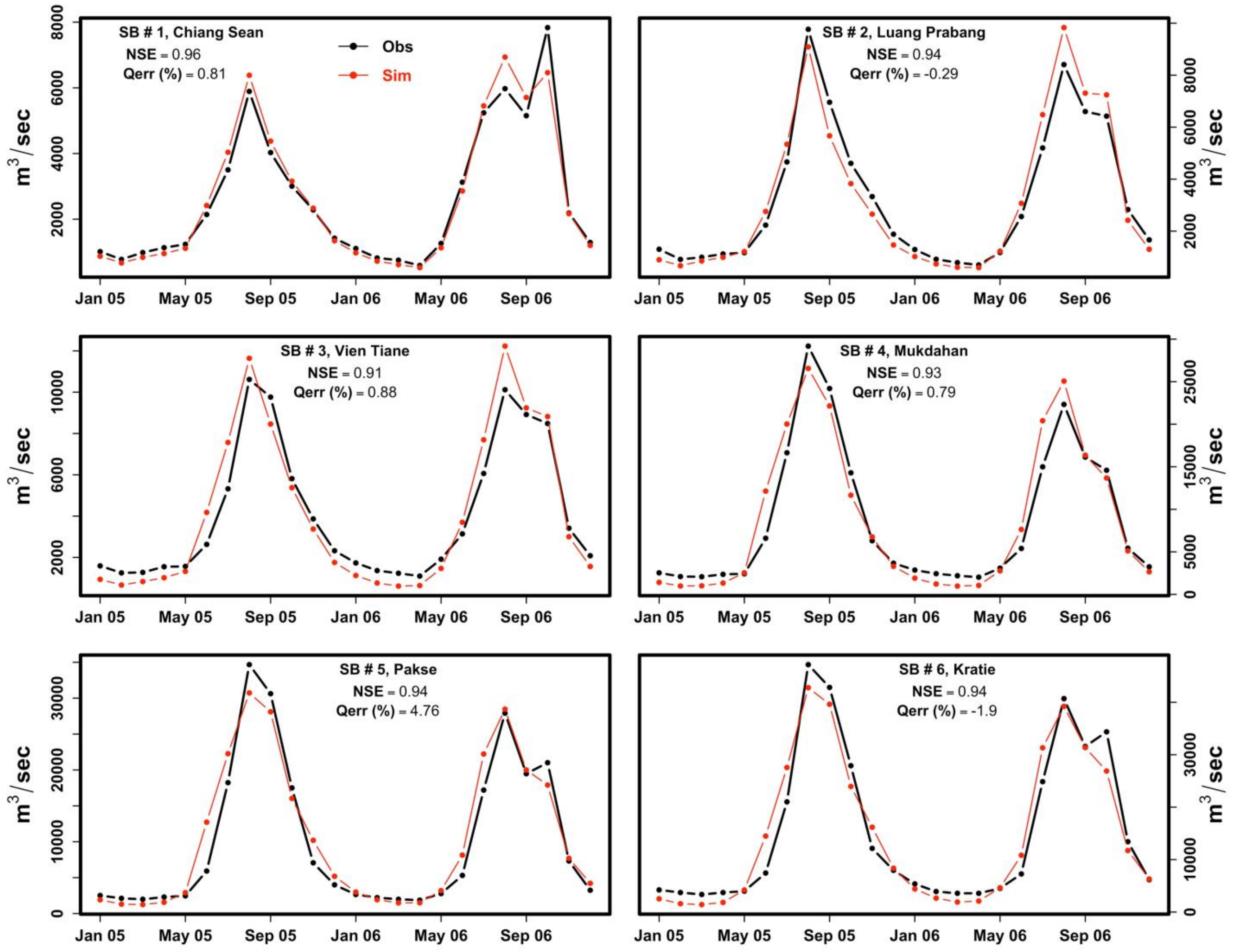

Mohammed, I. N., Bolten, J., Srinivasan, R., & Lakshmi, V. (2018). Improved Hydrological Decision Support System for the Lower Mekong River Basin Using Satellite-Based Earth Observations. Remote Sensing, 10(6), 885. http://dx.doi.org/10.3390/rs10060885

Remote Sensing and Gauge Driven SWAT Models – Streamflow Comparison

Sub Basin #	NSE (RS Driven Model)	NSE (In-Situ Driven Model)
SB#1 Chiang Sean	0.96	0.91
SB#2 Luang Prabang	0.94	0.70
SB#3 Vien Tiane	0.91	0.75

Sub Basin #	Qerr % (RS Driven Model)	Qerr % (In-Situ Driven Model)
SB#1 Chiang Sean	0.81	0.53
SB#2 Luang Prabang	-0.29	2.02
SB#3 Vien Tiane	0.88	-3.31

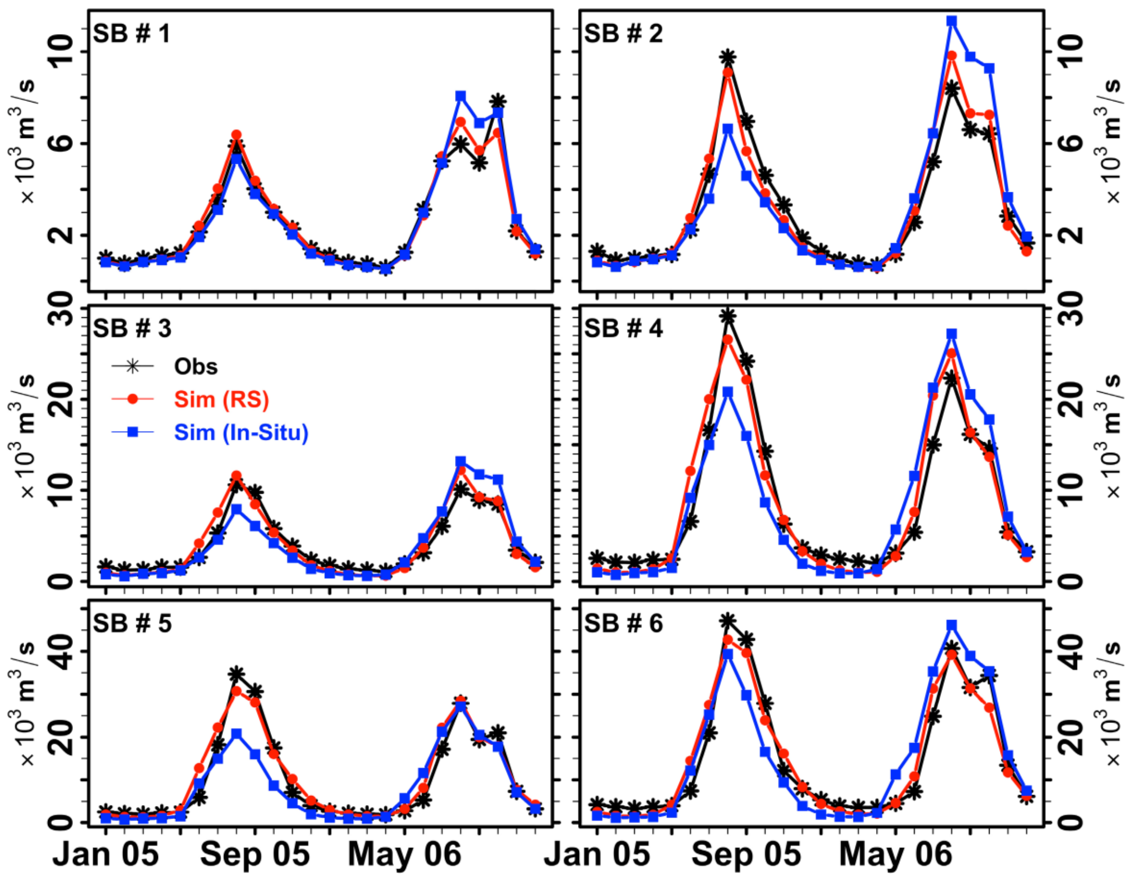

Monthly mean observed and simulated discharge in m^3/s at six sub-basin watersheds in calibration of the LMRB model (TRMM)

Mohammed, I. N., Bolten, J., Srinivasan, R., & Lakshmi, V. (2018). Improved Hydrological Decision Support System for the Lower Mekong River Basin Using Satellite-Based Earth Observations. Remote Sensing, 10(6), 885. http://dx.doi.org/10.3390/rs10060885

Remote Sensing (GPM) & LMRB SWAT Model

- The GPM-IMERG precipitation data used to drive the LMRB model for verification
- The SWAT model is able to explain between 71% and 96% of the variance observed in the monthly discharge from Chiang Sean, Thailand, to Kratie, Cambodia, when driven by GPM-IMERG

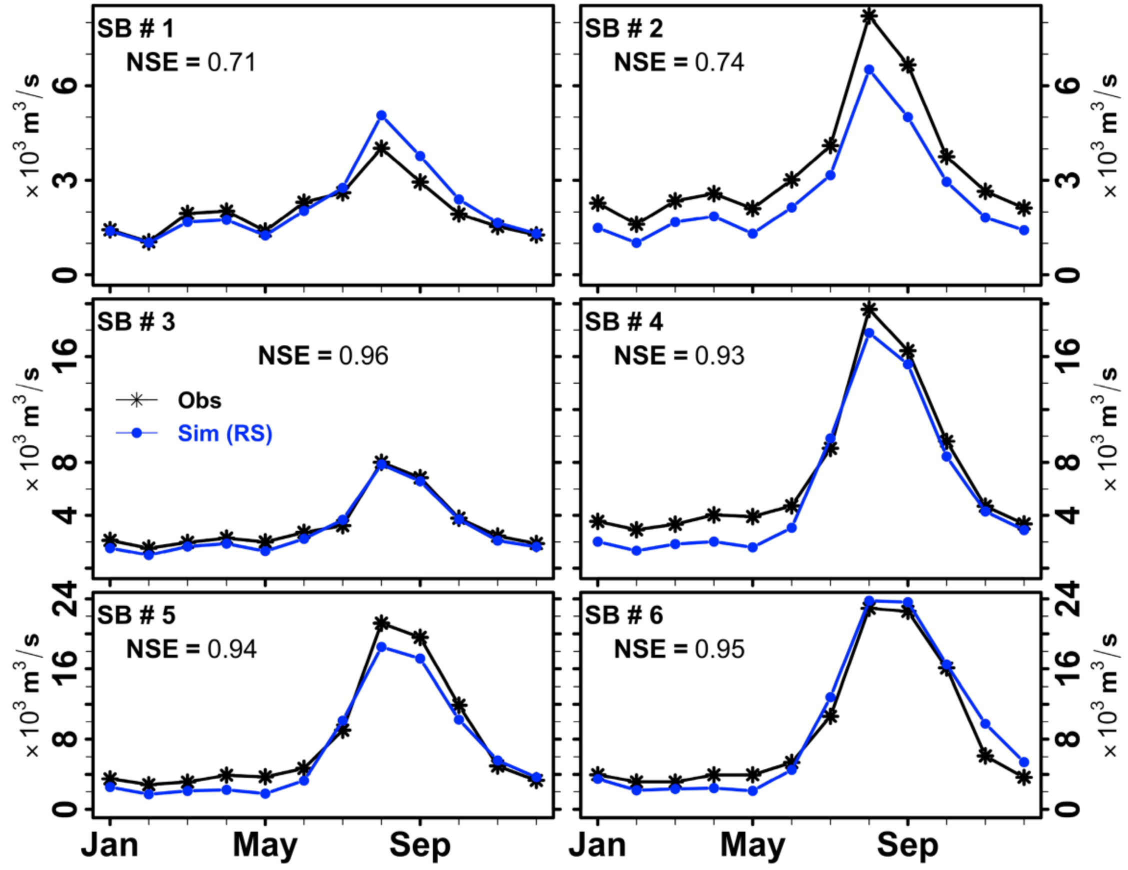

Monthly mean observed and simulated discharge in m^3/s at six sub-basin watersheds in calibration of the LMRB model (TRMM)

Mohammed, I. N., Bolten, J., Srinivasan, R., & Lakshmi, V. (2018). Improved Hydrological Decision Support System for the Lower Mekong River Basin Using Satellite-Based Earth Observations. Remote Sensing, 10(6), 885. http://dx.doi.org/10.3390/rs10060885

Le, H., J. Sutton, D. Bui, J. Bolten, and V. Lakshmi. 2018. "Comparison and Bias Correction of TMPA Precipitation Products over the Lower Part of Red–Thai Binh River Basin of Vietnam." Remote Sensing, 10 (10): 1582 [10.3390/rs10101582]

Lower Mekong River Basin Streamflow Variability Change

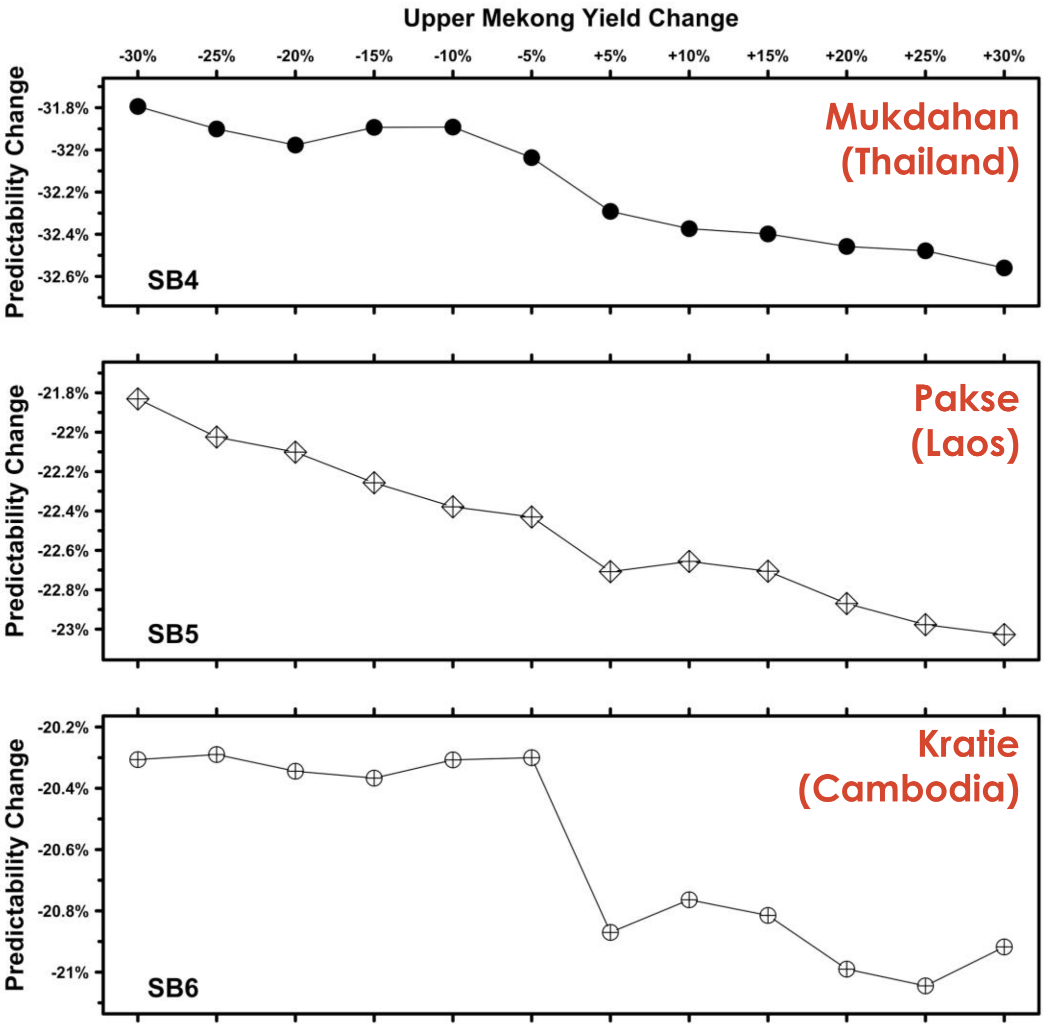

- Sensitivity analysis for the Lower Mekong River Basin Colwell index predictability (*P*)
- Observed predictability during 2001-2015 time period at SB4, SB5, and SB6 is 0.342, 0.325, and 0.317 respectively
- Predictability change (y-axis) reports the scaled predictability change, i.e., $(P_{sim} - P_{obs})/P_{obs} \times 100$

Mohammed, I.N., Bolten, J.D., Srinivasan, R., Lakshmi, V., 2018. Satellite observations and modeling to understand the Lower Mekong River Basin streamflow variability. J. Hydrol. 564, 559- 573, https://doi.org/10.1016/j.jhydrol.2018.07.030

High Flow Disturbance Analysis

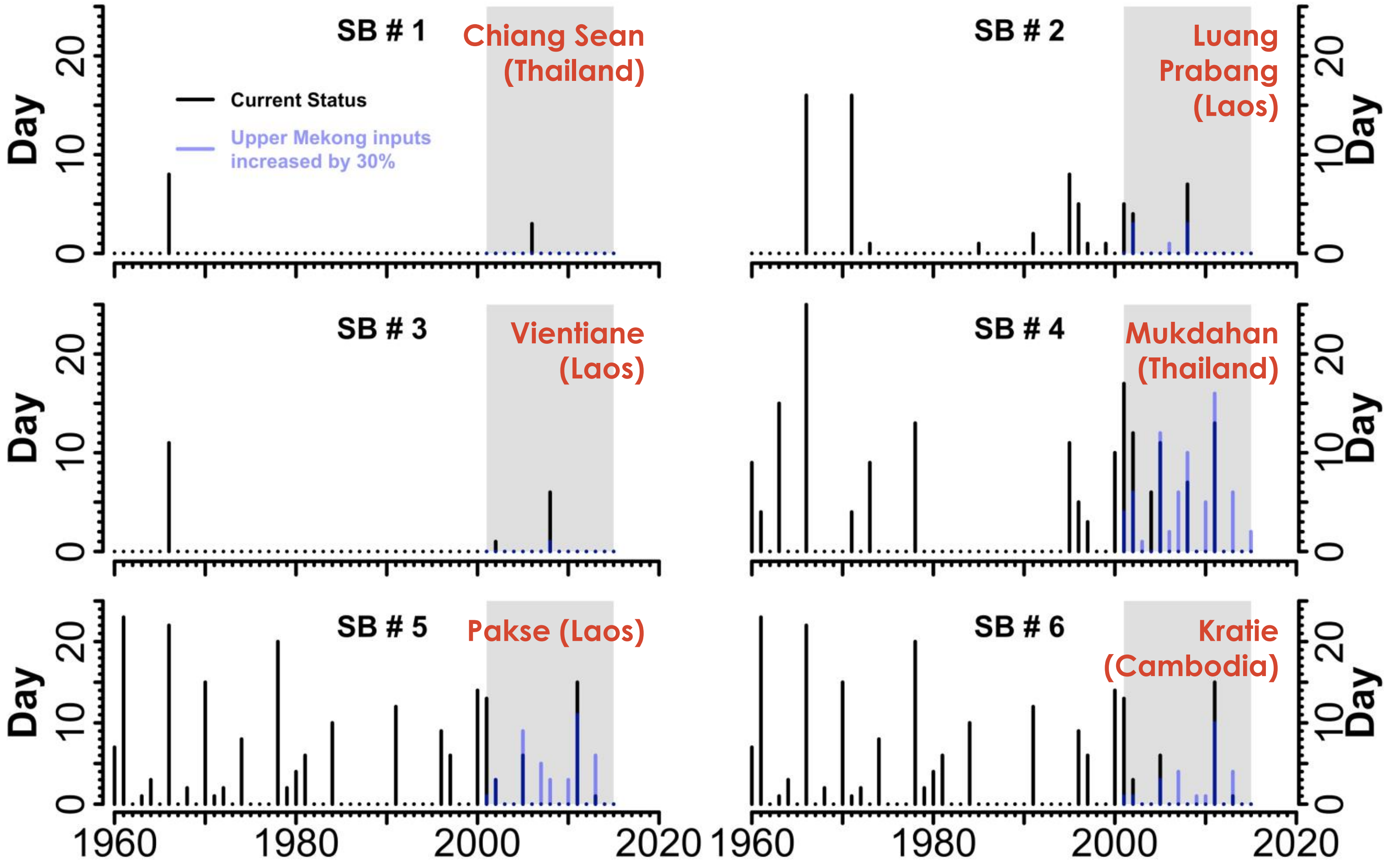

Mohammed, I.N., Bolten, J.D., Srinivasan, R., Lakshmi, V., 2018. Satellite observations and modeling to understand the Lower Mekong River Basin streamflow variability. J. Hydrol. 564, 559-573, https://doi.org/10.1016/j.jhydrol.2018.07.030

NASAaccess – Downloading & Reformatting Tool for NASA Earth Observation Data Products

GLDASpolyCentroid

Generate air temperature input files as well as air temperature stations file from NASA GLDAS modeled remote sensing products.

GPMpolyCentroid

Generate rainfall input files as well as rain station file from NASA GPM remote sensing products.

GLDASwat

Generate SWAT air temperature input files as well as air temperature stations file from NASA GLDAS modeled remote sensing products.

GPMswat

Generate SWAT rainfall input files as well as rain stations file from NASA GPM remote sensing products.

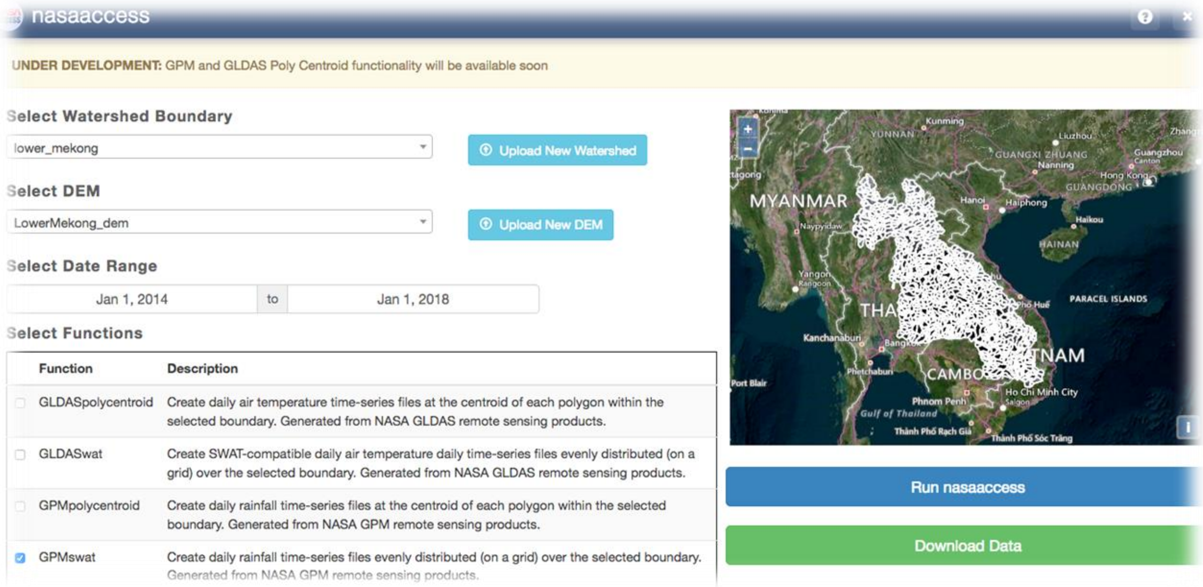

http://tethys-servir.adpc.net/apps/nasaaccess2/

Mohammed, I.N., Bolten, J., Srinivasan, R., Lakshmi, V., 2018. Improved hydrological decision support system for the Lower Mekong River Basin using satellite-based earth observations. Remote Sens. 10, 885, https://doi.org/10.3390/rs10060885

NASA Access has been officially released by NASA on its Github terminal

https://github.com/nasa/NASAaccess

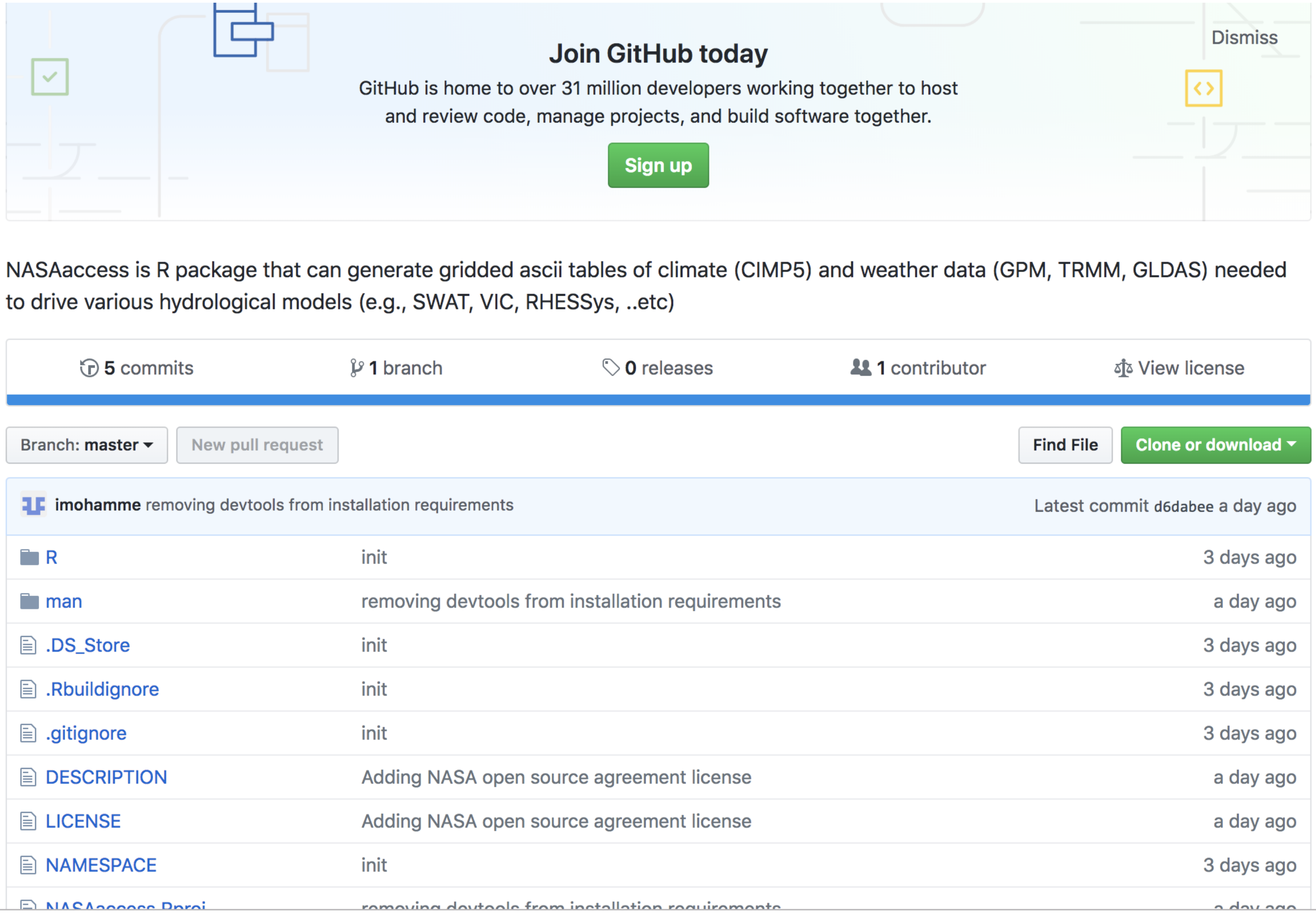

Examining Reservoir Scenarios

- **Baseline (December 2016)** – this is the same as Regan et al's, (n.d.) Baseline development scenario
- **Current (October 2018)** – the baseline scenario plus the now commissioned lower Sesan II and completed Nam Kong 2 reservoir in Laos
- **Under contract/construction** – includes the previous scenarios plus the dams that are at the stage of on-ground works. This includes Upper Kontum, Nam Kong 3, Xe Nam Noy 2 - Xe Katam 1
- **Contracted/licensed** – this includes the dams in the previous scenarios and dams listed as licensed by the MRC: Xe Katam; Xekong 4; Nam Kong 1 and Xe Kaman 4
- **Lower Sekong** – Under contract/construction plus lower Sekong
- **Lower Srepok 3** – Under contract/construction plus Lower Srepok 3
- **Cambodia Sesan and Srepok** – An alternative to the lower Sekong. Under construction plus Lower Srepok 3, lower Sesan 3 and lower Srepok 2

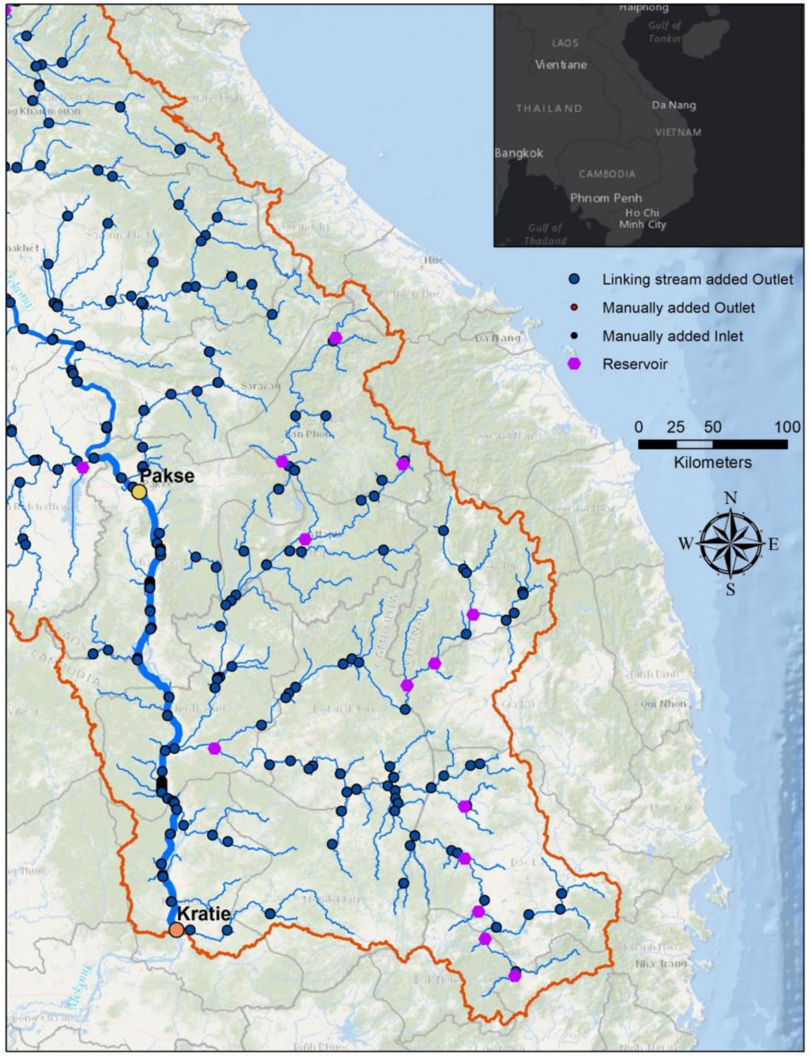

Near Real-Time Flood Damage Assessment

From Data to Decisions

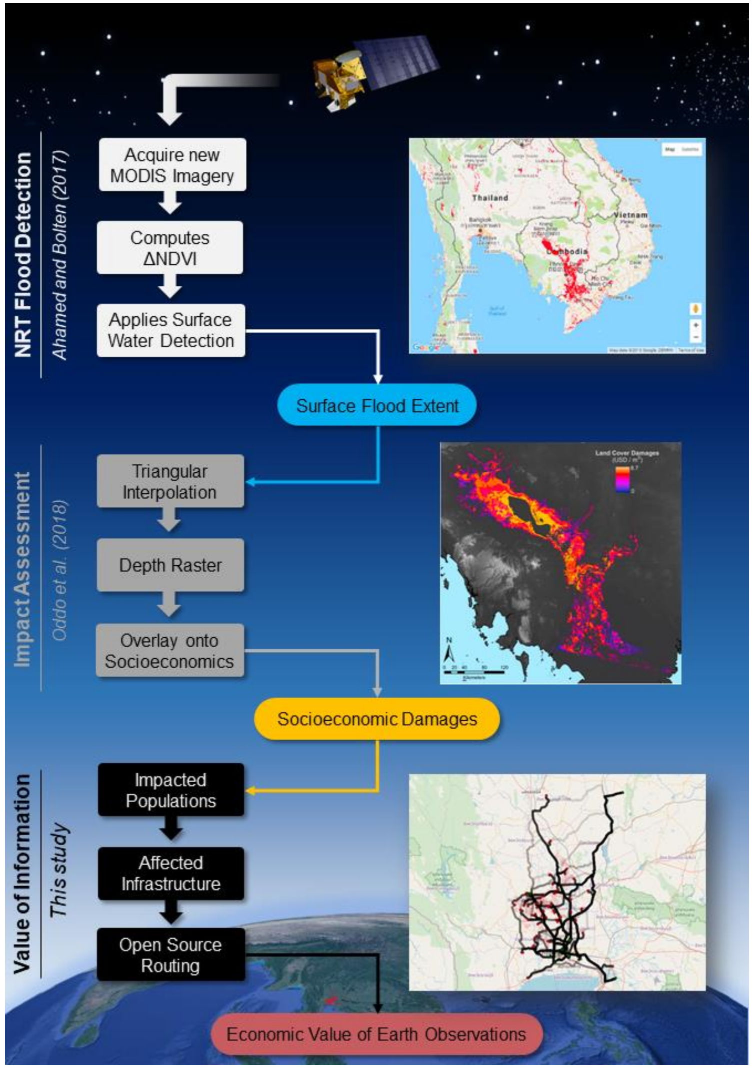

Fayne, J. V., J. D. Bolten, C. S. Doyle, et al. 2017. "Flood mapping in the lower Mekong River Basin using daily MODIS observations." International Journal of Remote Sensing, 38 (6): 1737-1757 [10.1080/01431161.2017.1285503]
Ahamed, A., and J. Bolten. 2017. "A MODIS-based automated flood monitoring system for southeast asia." International Journal of Applied Earth Observation and Geoinformation, 61: 104-117 [10.1016/j.jag.2017.05.006]
Ahamed, A., J. D. Bolten, C. Doyle, and J. Fayne. 2016. "Near Real-Time Flood Monitoring and Impact Systems." Remote Sensing of Hydrological Extremes, 105-118 [10.1007/978-3-319-43744-6]
Fayne, J., J. Bolten, V. Lakshmi, and A. Ahamed. 2016. "Optical and Physical Methods for Mapping Flooding with Satellite Imagery."Remote Sensing of Hydrological Extremes, 83-103 [10.1007/978-3-319-43744-6_5]

Validation Summary

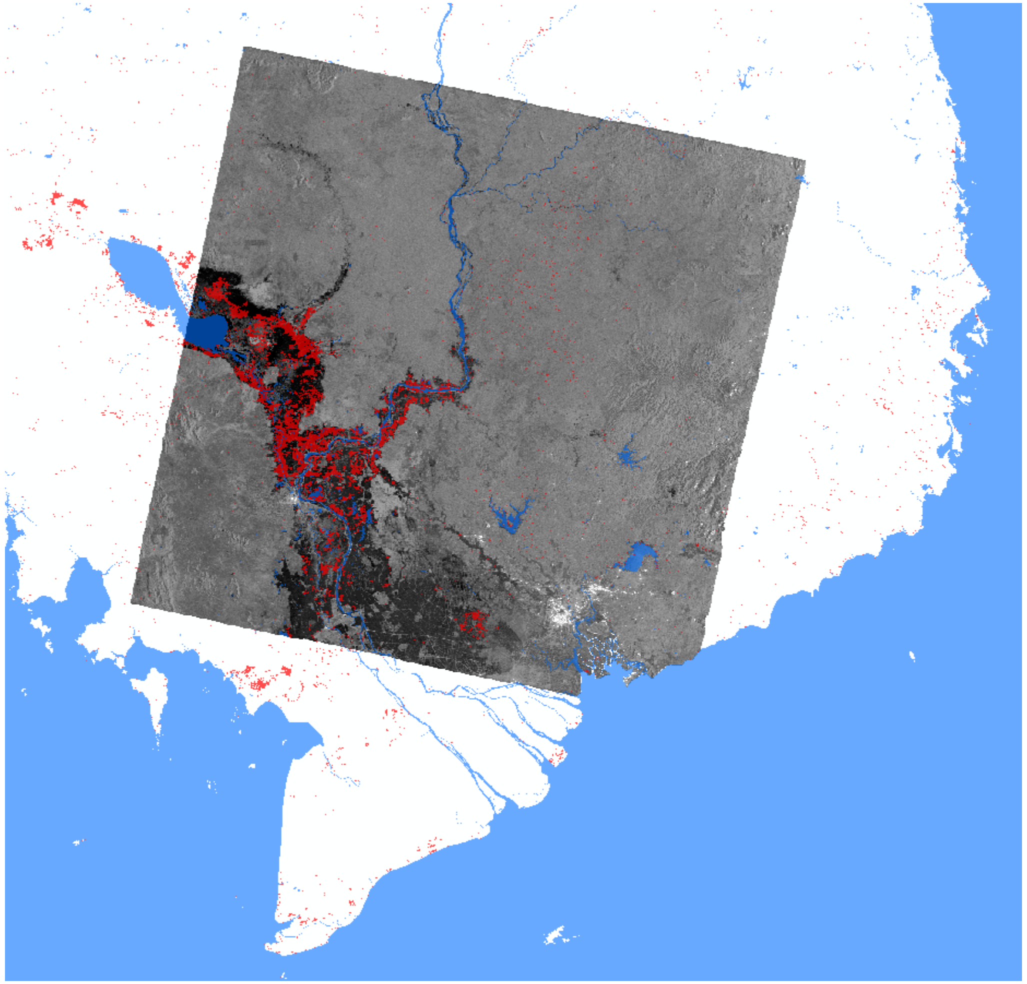

- **Overall accuracy :** 87%
- **Pixels analyzed:** > 7 million
- **Accuracy Range:** 79% - 98%
- **Conditions:** Flood, Non – Flood
- **Sensors:** (1) Envisat ASAR, (2) Radarsat – 2, (3) TerraSAR-X, (4) Disaster Monitoring Constellation (DMC)

Ahamed, A., and J. Bolten. 2017. "A MODIS-based automated flood monitoring system for southeast asia." International Journal of Applied Earth Observation and Geoinformation, 61: 104-117 [10.1016/j.jag.2017.05.006]

Near Real-Time Flood Inundation Mapping

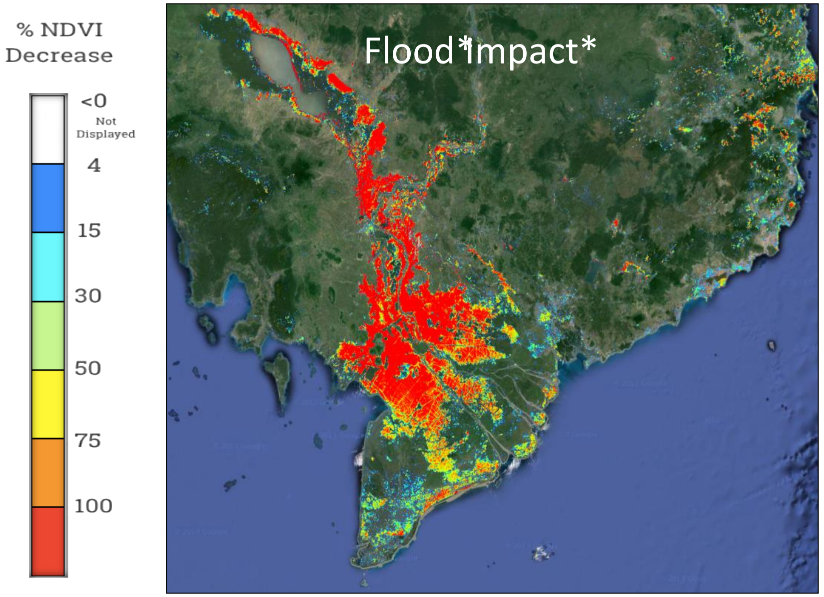

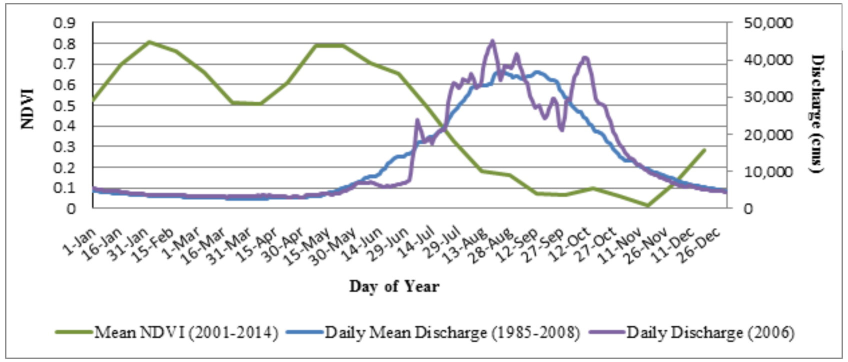

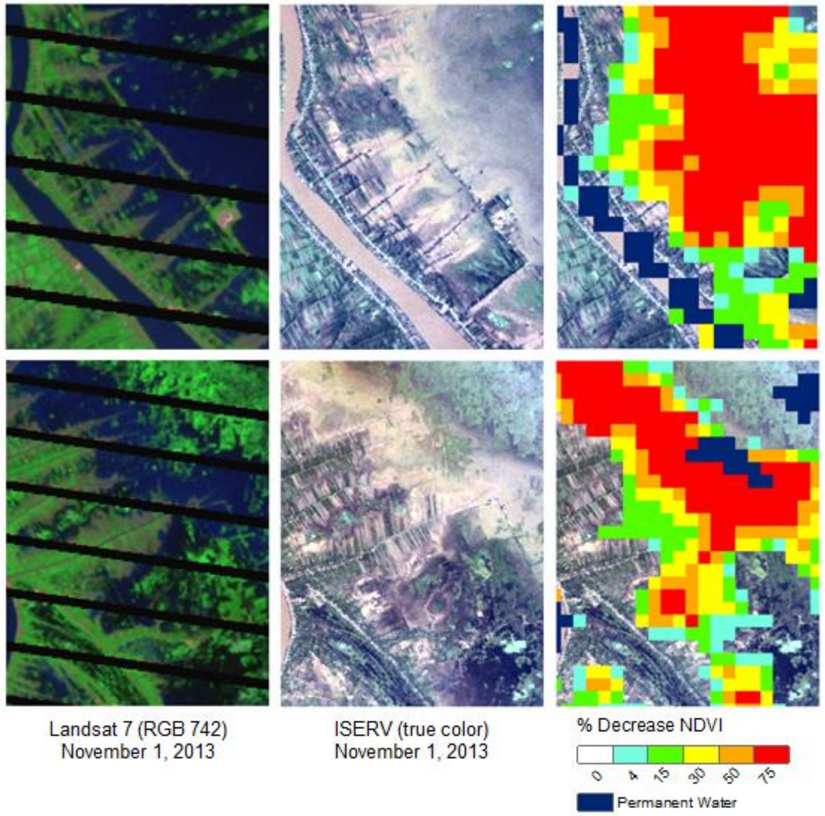

Operational Near Real-Time Flood Inundation maps based on relative anomalies in NDVI from MODIS 250-m data

Stakeholders: Mekong River Commission

Doyle, C., J. Boten, J. Spruce, "Flood Inundation Mapping in the Lower Mekong River Basin Using Multi-Temporal MODIS Observations," IEEE J. Sel. Topics Appl. Earth Observ. in Remote Sens. (in review)

Near Real-Time Flood Inundation Mapping

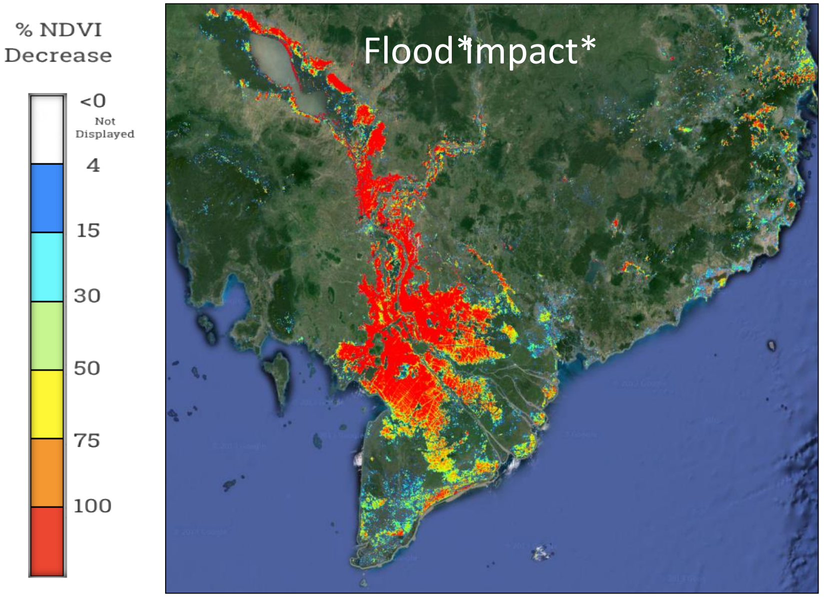

Reference Data	Date	Overall Accuracy	Kappa
ISERV	1-Nov 2013 (n = 200)	88.50%	0.77
Landsat 7 ETM+	1-Nov 2013 (n = 300)	94.00%	0.88

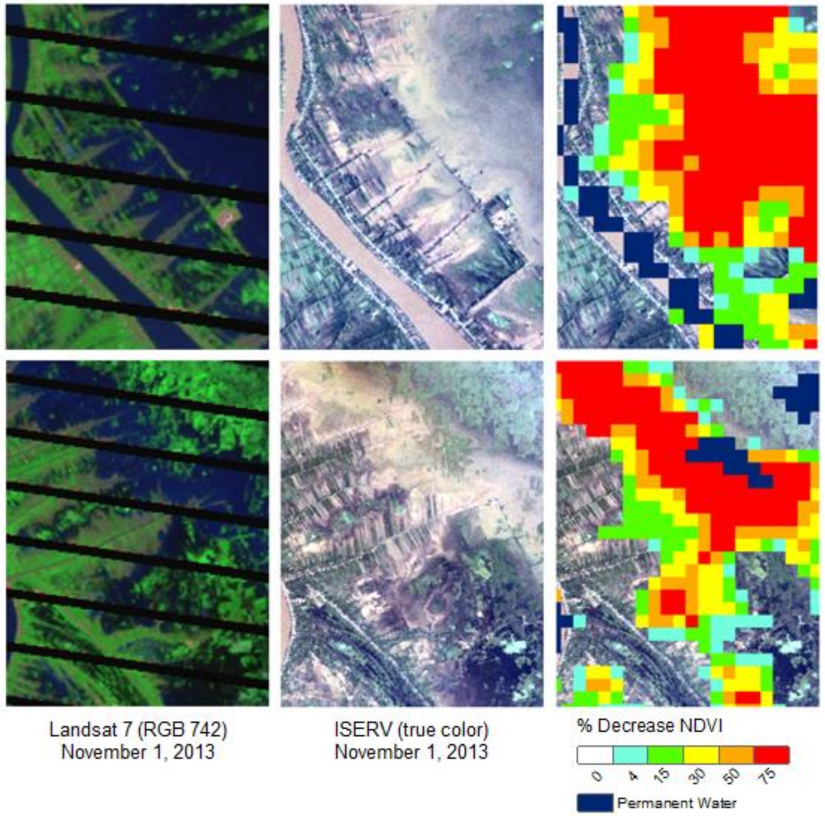

Operational Near Real-Time Flood Inundation maps based on relative anomalies in NDVI from MODIS 250-m data

Stakeholders: Mekong River Commission

Doyle, C., J. Boten, J. Spruce, "Flood Inundation Mapping in the Lower Mekong River Basin Using Multi-Temporal MODIS Observations," IEEE J. Sel. Topics Appl. Earth Observ. in Remote Sens. (in review)

Damage Framework

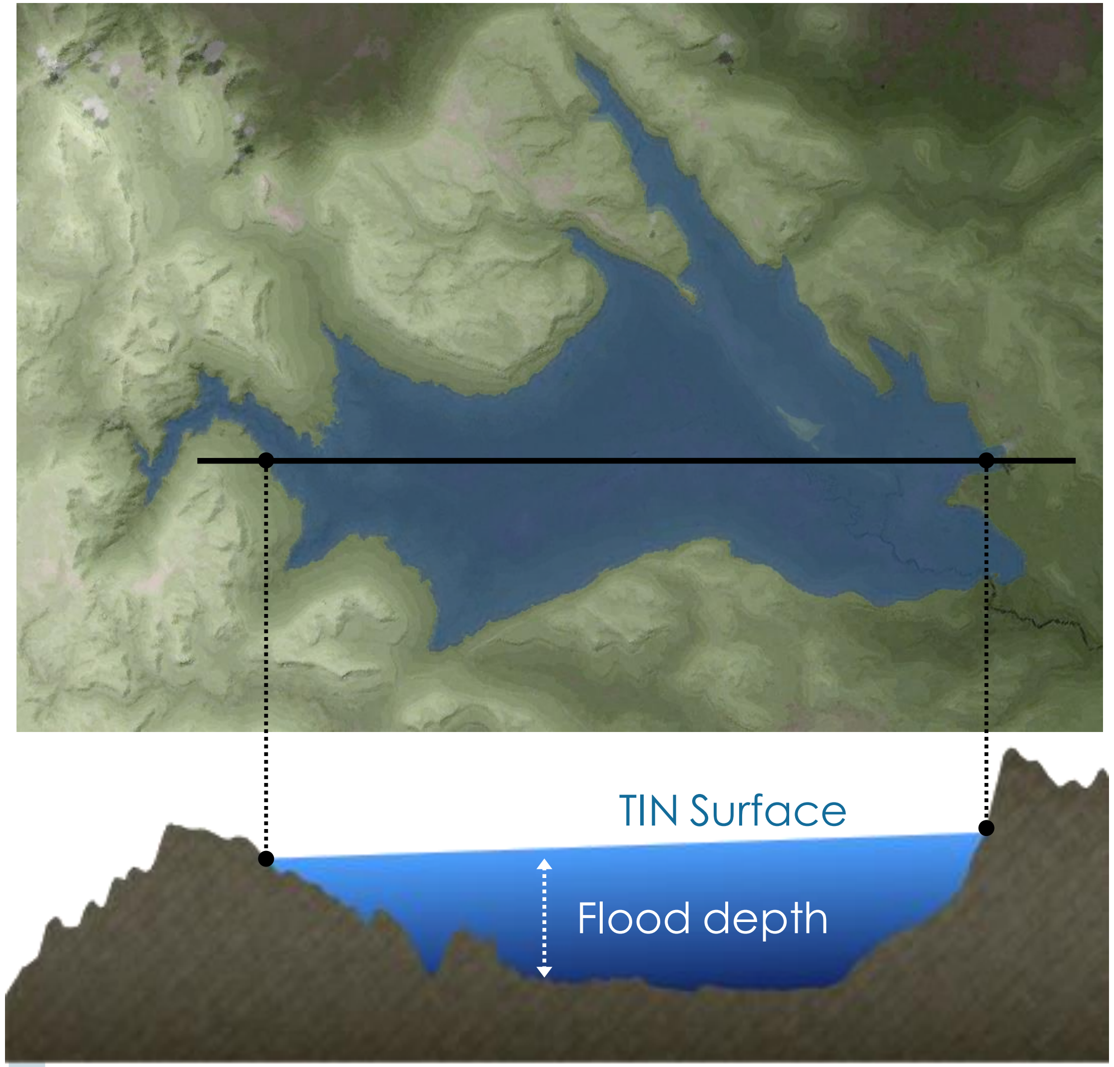

Flood Depth Estimations

- Apply method from Cham et al. (2015)*
- Extract flood extent from detection tool
- Generate points around the perimeter
  – Sample elevation values from DEM
- Produce Triangulated irregular Network (TIN) to visualize water surface elevation

Oddo, P., A. Ahamed, and J. Bolten. 2018. "Socioeconomic Impact Evaluation for Near Real-Time Flood Detection in the Lower Mekong River Basin." Hydrology, 5 (2): 23 [10.3390/hydrology5020023]
* Cham, T. C., Mitani, Y., Fujii, K. & Ikemi, H. Evaluation of flood volume and inundation depth by GIS midstream of Chao Phraya River Basin, Thailand. in WIT Transactions on The Built Environment (ed. Brebbia, C. A.) 1, 1049–1060 (WIT Press, 2015).

Damage Framework

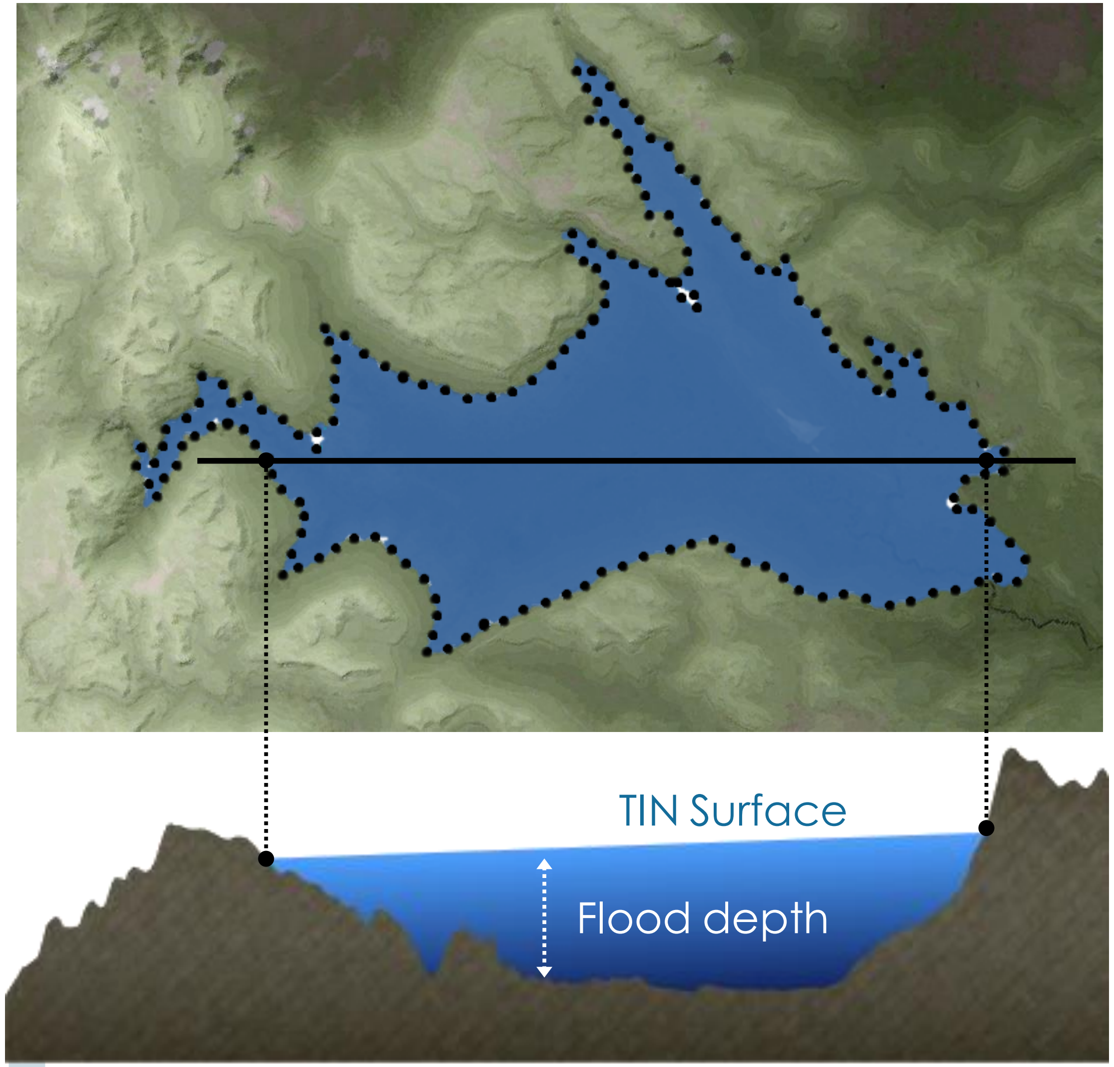

Flood Depth Estimations

- Apply method from Cham et al. (2015)*
- Extract flood extent from detection tool
- Generate points around the perimeter
  – Sample elevation values from DEM
- Produce Triangulated irregular Network (TIN) to visualize water surface elevation

Oddo, P., A. Ahamed, and J. Bolten. 2018. "Socioeconomic Impact Evaluation for Near Real-Time Flood Detection in the Lower Mekong River Basin." Hydrology, 5 (2): 23 [10.3390/hydrology5020023]
* Cham, T. C., Mitani, Y., Fujii, K. & Ikemi, H. Evaluation of flood volume and inundation depth by GIS midstream of Chao Phraya River Basin, Thailand. in WIT Transactions on The Built Environment (ed. Brebbia, C. A.) 1, 1049–1060 (WIT Press, 2015).

Damage Framework

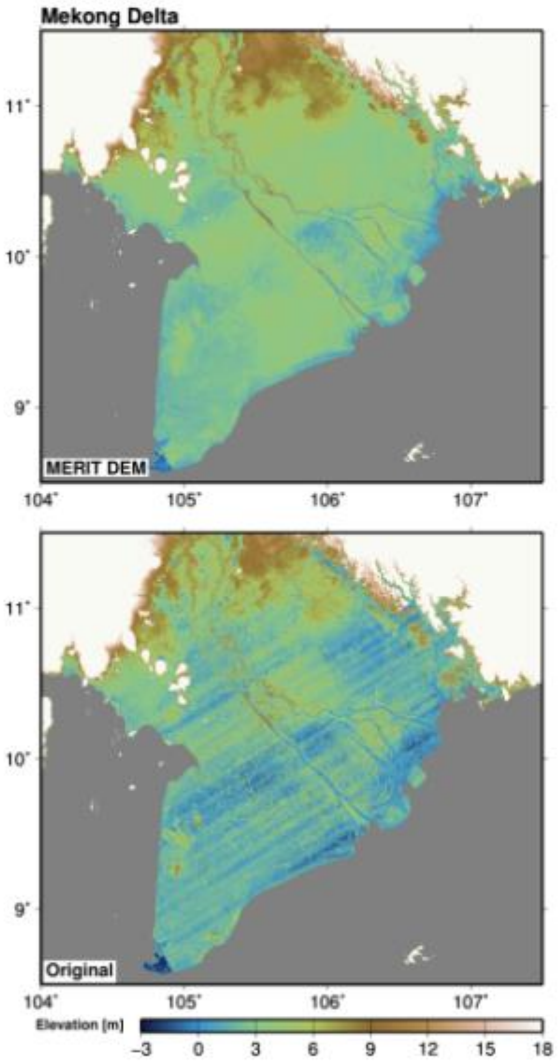

Flood Depth Estimations

- Utilizes improved Multi-Error-Removed Improved-Terrain (MERIT) DEM[6]
- ~20% increase in land area mapped with 2-meter or better vertical accuracy

6. Yamazaki, D., Ikeshima, D., Tawatari, R., Yamaguchi, T., O'Loughlin, F., Neal, J. C., … Bates, P. D. (2017). A high-accuracy map of global terrain elevations. Geophysical Research Letters, 44(11), 2017GL072874. https://doi.org/10.1002/2017GL072874

Location & Objectives

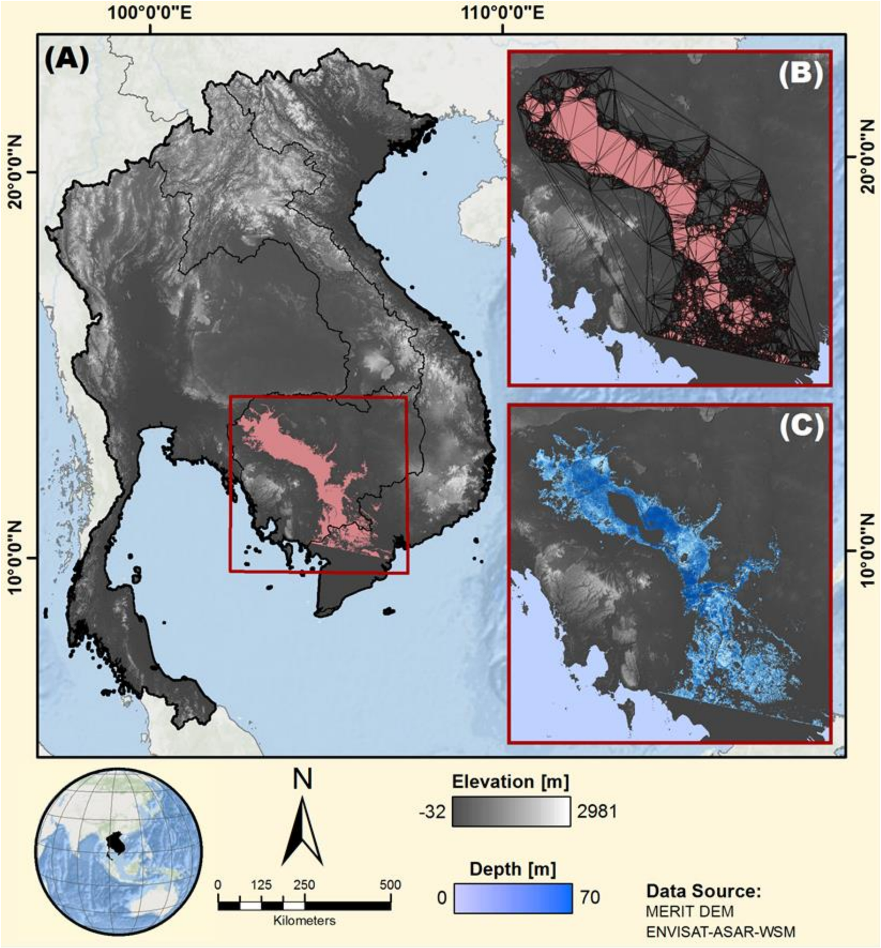

Figure 1. (**A**) Map of Mekong River Basin countries with flood extent from 2011 event. (**B**) Study extent showing results of the triangular interpolated network (TIN). (**C**) Depth raster produced by inundation depth analysis.

2011 Southeast Asia Floods

- La Niña event – 143% increase in rainfall
- Onset of southwest monsoon

Objectives

- Use 2011 flood event as case study to demonstrate feasibility
- Integrate framework into Project Mekong near real-time platform

Oddo, P., A. Ahamed, and J. Bolten. 2018. "Socioeconomic Impact Evaluation for Near Real-Time Flood Detection in the Lower Mekong River Basin." Hydrology, 5 (2): 23 [10.3390/hydrology5020023]

Land Cover / Land Use

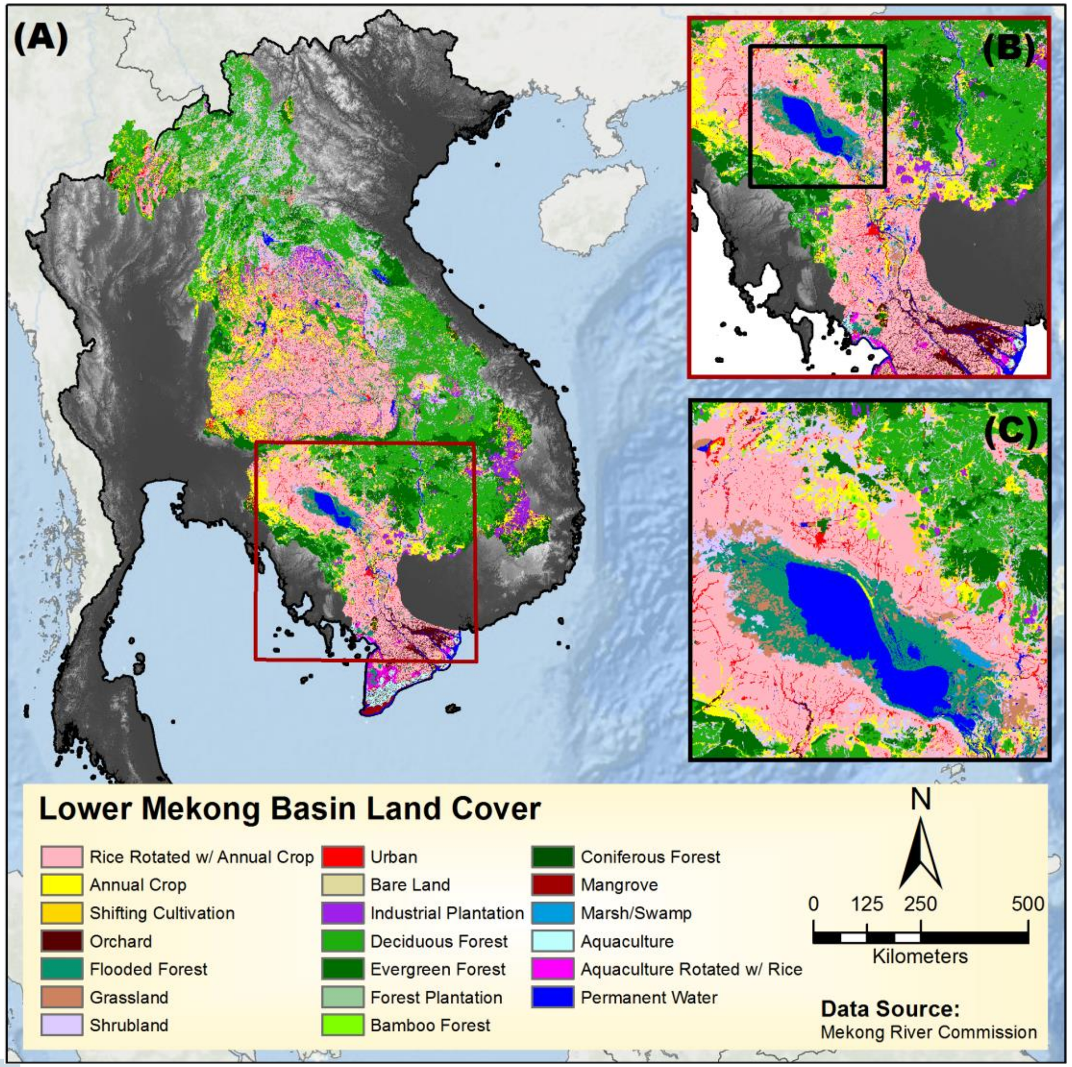

Updated Land Cover

- Produced by MRC (2010)
- Landsat-5 derived at 30 m resolution
- 19 unique land cover classifications
- 9,357 survey points collected for validation

Figure 3. (**A**) Land use/land cover (LULC) map produced by Mekong River Commission (MRC, 2010). (**B**) Inset showing study extent and LULC details considered in this analysis. (**C**) Close view of the Tonle Sap Lake region, Cambodia.

Population / Infrastructure

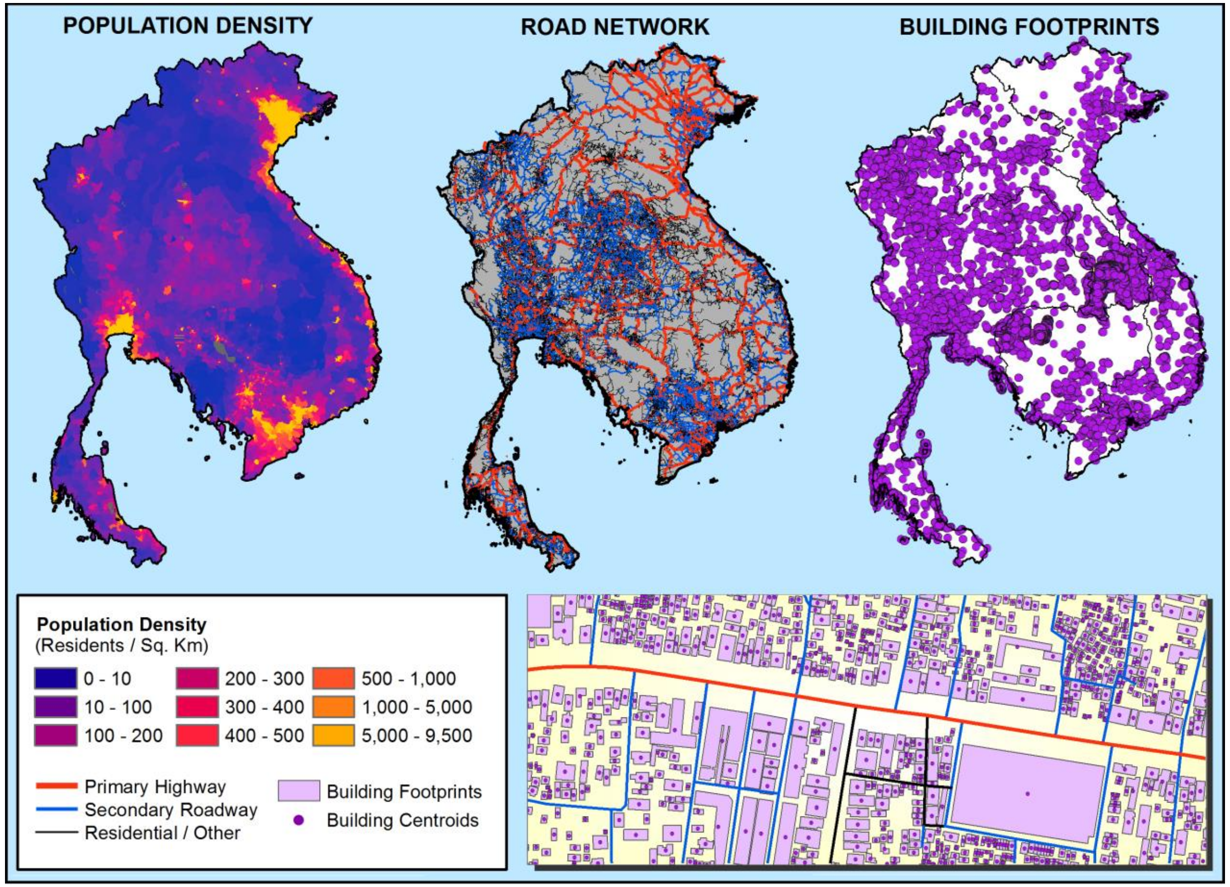

Figure 4. Population density (**left**), regional road networks (**center**), and building centroid and footprint data (**right, below**) considered in this study.

Socioeconomic Data

- NASA Socioeconomic Data and Applications Center (SEDAC)
  – Gridded population density (GPW)
  – Global gridded roads (gROADS)

Open Source Data

- Building location (centroids) and footprints:
  – OpenStreetMaps

Oddo, P., A. Ahamed, and J. Bolten. 2018. "Socioeconomic Impact Evaluation for Near Real-Time Flood Detection in the Lower Mekong River

Damage Calculations

0	0	1	2	2	3
1	3	2	1	2	5
0	5	4	1	1	2
0	1	0	2	2	3
1	2	5	5	3	4
1	2	3	4	5	5

Depth (m)

1	1	2	4	5	5
2	1	1	4	5	5
2	1	1	4	5	7
2	5	5	5	5	7
5	5	6	6	7	9
5	6	6	6	8	9

Land Use Category	
1	Rice - 1 crop/yr
2	Mixed Annual Crops
3	Cleared before 2010
4	Orchard
5	Flooded Forest
6	Grassland/Sparse Vegetation
7	Deciduous Shrubland
8	Urban
9	Barren - Rock Outcrops

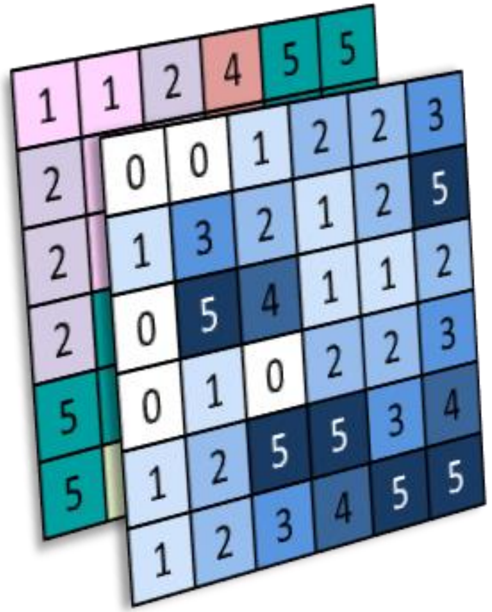

Oddo, P. C., Ahamed, A., & Bolten, J. D. (2018). Socioeconomic Impact Evaluation for Near Real-Time Flood Detection in the Lower Mekong River Basin. Hydrology, 5(2), 23. https://doi.org/10.3390/hydrology5020023

Damage Model

"Standard Method"

$$S = \sum_{i=1}^{n} a_i n_i S_i$$

where

- a_i = damange factor category I
- n_i = number of units in category I
- S_i = maximum damage per unit in category i

Kok, M., Huizinga, H. J., Vrouwenfelder, A. & Barendregt, A. Standard method 2004. Damage and casualties caused by flooding. (Rijkswaterstaat, 2004).

Oddo, P. C., Ahamed, A., & Bolten, J. D. (2018). Socioeconomic Impact Evaluation for Near Real-Time Flood Detection in the Lower Mekong River Basin. Hydrology, 5(2), 23. https://doi.org/10.3390/hydrology5020023

Maximum Damage Values (S_i)

Land utility	USD/m²	Source
Agriculture		
Rice, totally destroyed	0.078	
Crop, totally destroyed	0.109	
Other Plants, totally destroyed	0.147	Leenders et al. (2009)
Rice, partially destroyed	0.027	
Crop, partially destroyed	0.030	
Other Plants, partially destroyed	0.030	
Fishery		
Farm. Ponds and paddy fields	0.639	
Shrimp and shell fish	1.706	Leenders et al. (2009)
Freshwater fish	0.048	
Infrastructure		
Urban area	29	
Rural area	22	
Provincial road	80	
National road	400	Giang et al. (2009)
Railway	1000	
Rice	0.044	
Other crops	0.02	
Forest	0.84	

Depth-Damage Curves

Damage Factor (a_i): General

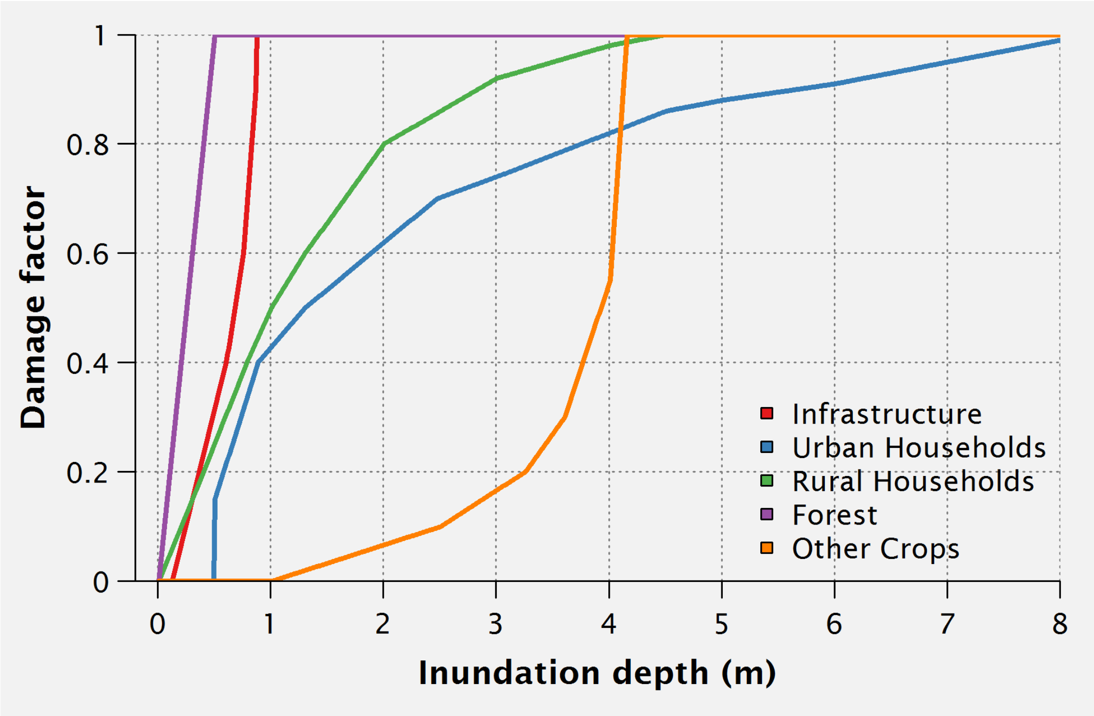

Damage Factor (a_i): Rice-Specific

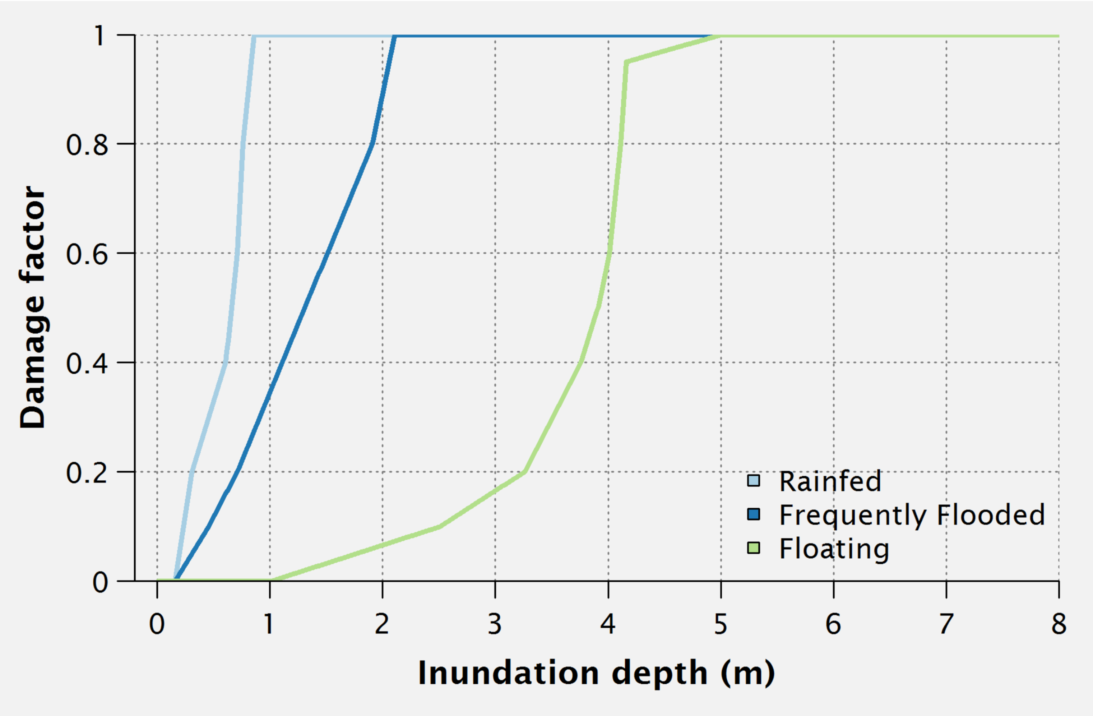

Figure 5. Damage factor curves for agriculture, forest, and infrastructure classes (**upper**) and rice varieties (**lower**) found in the Lower Mekong Basins (LMB). Curves digitized and adapted from Chen (2007) [49].

Oddo, P. C., Ahamed, A., & Bolten, J. D. (2018). Socioeconomic Impact Evaluation for Near Real-Time Flood Detection in the Lower Mekong River Basin. Hydrology, 5(2), 23. https://doi.org/10.3390/hydrology5020023

Visualizing Impacts

Land Utility	Area (km²)	Damages (USD)
Rice Rotated with Annual Crop	13,355.05	645,235,056
Annual Crop	1502.03	126,696,853
Shifting Cultivation	38.02	3,073,550
Orchard	332.35	6,572,509
Flooded Forest	3542.54	2,889,181,644
Grassland	1938.22	44,535,518
Shrub Land	1398.63	34,103,750
Urban	275.17	710,538,630
Bare Land	68.65	0
Industrial Plantation	1.42	24,608
Deciduous Forest	8.43	2,905,977
Evergreen Forest	2.28	1,530,465
Forest Plantation	-	-
Bamboo Forest	11.35	8,798,317
Coniferous Forest	-	-
Mangrove	1.71	842,254
Marsh/Swamp	482.85	12,703,670
Aquaculture	8.32	211,169
Aquaculture Rotated with Rice	26.39	27,770
Total	22,993	4,486,981,740

Oddo, P. C., Ahamed, A., & Bolten, J. D. (2018). Socioeconomic Impact Evaluation for Near Real-Time Flood Detection in the Lower Mekong River Basin. Hydrology, 5(2), 23. https://doi.org/10.3390/hydrology5020023

Visualizing Impacts

Land Utility	Area (km²)	Damages (USD)
Rice Rotated with Annual Crop	13,355.05	645,235,056
Annual Crop	1502.03	126,696,853
Shifting Cultivation	38.02	3,073,550
Orchard	332.35	6,572,509
Flooded Forest	3542.54	2,889,181,644
Grassland	1938.22	44,535,518
Shrub Land	1398.63	34,103,750
Urban	275.17	710,538,630
Bare Land	68.65	0
Industrial Plantation	1.42	24,608
Deciduous Forest	8.43	2,905,977
Evergreen Forest	2.28	1,530,465
Forest Plantation	-	-
Bamboo Forest	11.35	8,798,317
Coniferous Forest	-	-
Mangrove	1.71	842,254
Marsh/Swamp	482.85	12,703,670
Aquaculture	8.32	211,169
Aquaculture Rotated with Rice	26.39	27,770
Total	22,993	4,486,981,740

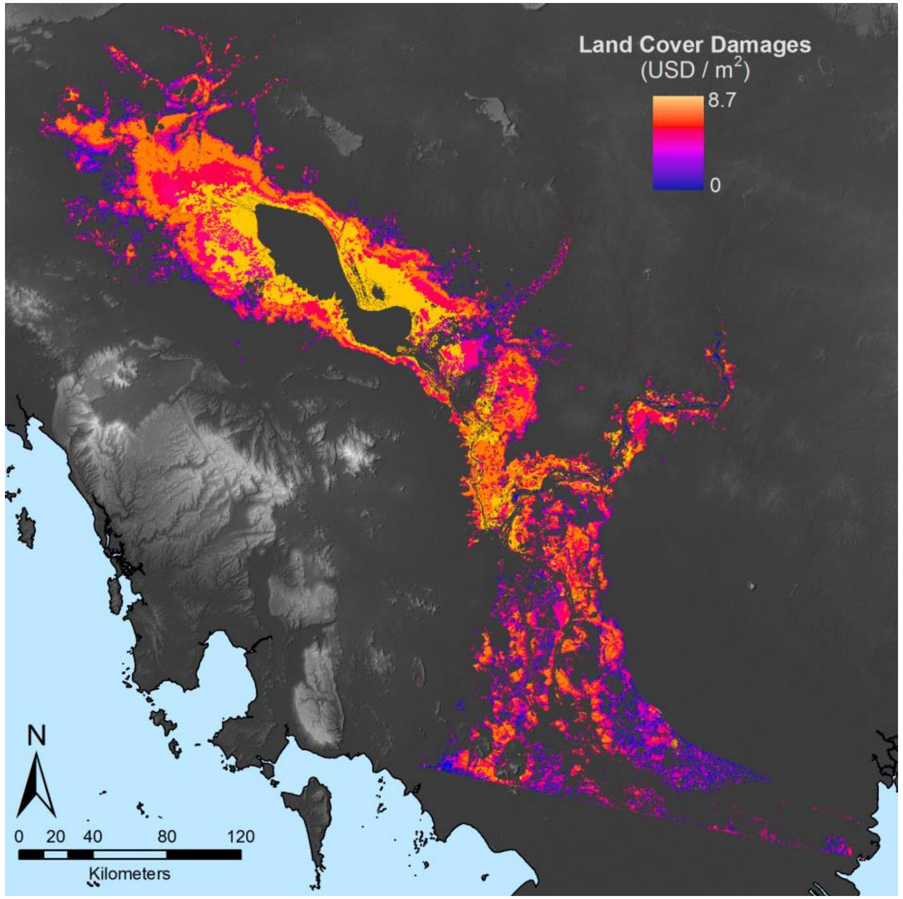

Figure 6. Results of damage assessment for land cover categories. Color gradient represents severity of damages in USD/m^2.

Oddo, P. C., Ahamed, A., & Bolten, J. D. (2018). Socioeconomic Impact Evaluation for Near Real-Time Flood Detection in the Lower Mekong River Basin. Hydrology, 5(2), 23. https://doi.org/10.3390/hydrology5020023

Limitation of Current System > Future Work

Updated Data

- Socioeconomic datasets
- Locally-specific valuations
- Improved geospatial information

Feedback

- What information is useful?
- How would it be used?

	Direct	Indirect

Tangible	• Damage to infrastructure
	  • Global roads
	  • Energy infrastructure
	  • Schools & hospitals
	  • Building footprints
	• Impacts to populations
		• Agricultural production
		• Income loss from industry/tourism
		• Emergency evacuation costs
		• Education disruption

Intangible	• Loss of human life • Biodiversity effects • Loss to ecosystem services (e.g., riparian vegetation) • Psychological suffering	• Impacts to place and culture • Community Resilience

Regional Workshop on Near Real-Time Flood Monitoring Service

Bangkok, Thailand (Jan 24-25, 2018)

Damage Assessment in Laos

Topics | Missions | Galleries | NASA TV | Follow NASA | Downloads | About | NASA Audiences | Search

Latest | Related

2015-2016 El Niño Triggered Disease Outbreaks Across Globe
5 days ago

On its 5th Anniversary, GPM Still Right as Rain
6 days ago

Help NASA Track and Predict Mosquito-Borne Disease Outbreaks
8 months ago

NASA Soil Moisture Data Advances Global Crop Forecasts
9 months ago

NASA Mapping Hurricane Damage to Everglades, Puerto Rico Forests
a year ago

NASA Visualizes the Dance of a Melting Snowflake
a year ago

Scientists Deploy Damage Assessment Tool in Laos Relief Efforts

The July 23 failure of the Xepian-Xe Nam Noy hydropower dam unleashed more than 130 billion gallons of water on rural villages in southern Laos, in Southeast Asia, devastating thousands of houses and businesses and displacing more than 6,000 people. As authorities scrambled to gather information in the wake of the disaster, scientists at NASA's Goddard Space Flight Center in Greenbelt, Maryland, activated a new tool to help them assess the damage and get help to people in need.

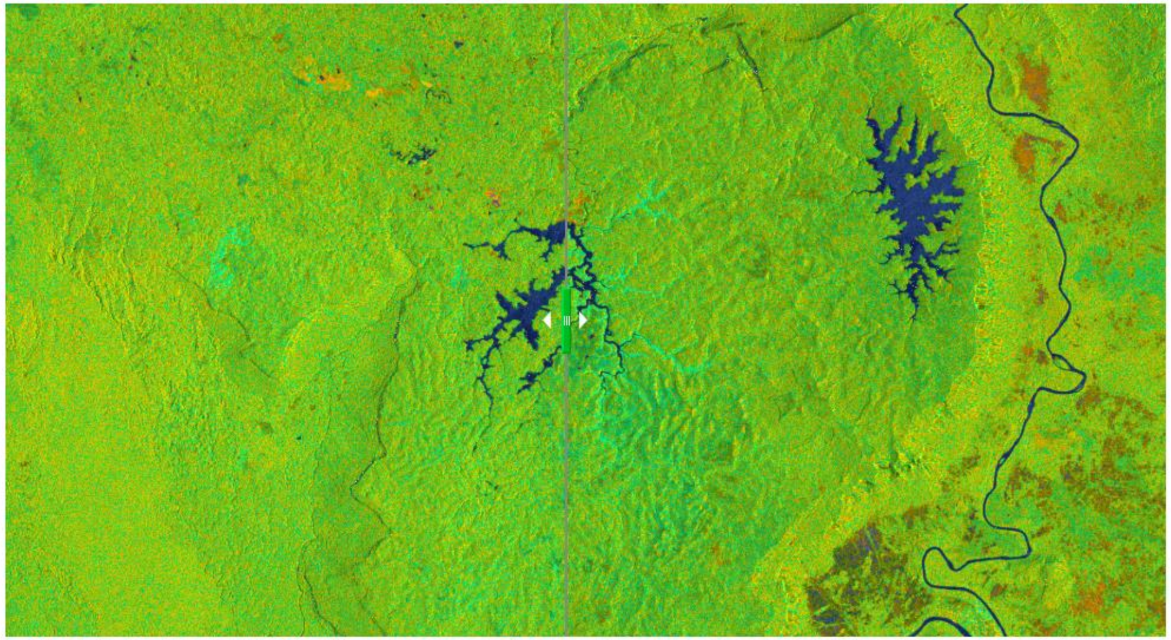

Show only Left | Show only Right

The Sentinel-1 satellite from the European Space Agency (ESA) Copernicus program observed the area surrounding the Xepian-Xe Nam Noy dam in Laos before (left) and after (right) the dam's July 23, 2018, failure. The left image is from July 17. In the right image, from July 25, the reservoir behind the dam has been significantly reduced in size, and the river downstream of the dam (to the left of the reservoir) is more apparent, with brown hues indicating potential flooding.

Credits: NASA Disasters/Marshall Space Flight Center/Alaska Satellite Facility; contains modified Copernicus Sentinel data (2018) processed by ESA

Flood Damage Assessment System Activated for July 25 Laos Dam Break

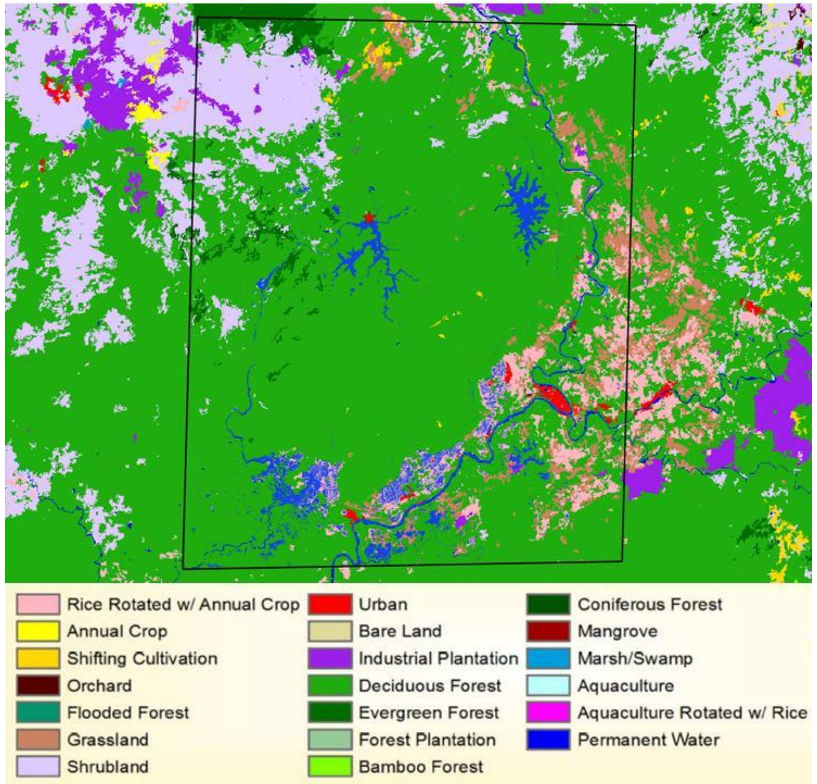

- **By the numbers**
- >3,740 people impacted
- 1,349 buildings
- 373 km of affected roads
- $54 million (USD) of potential damage to infrastructure and land cover

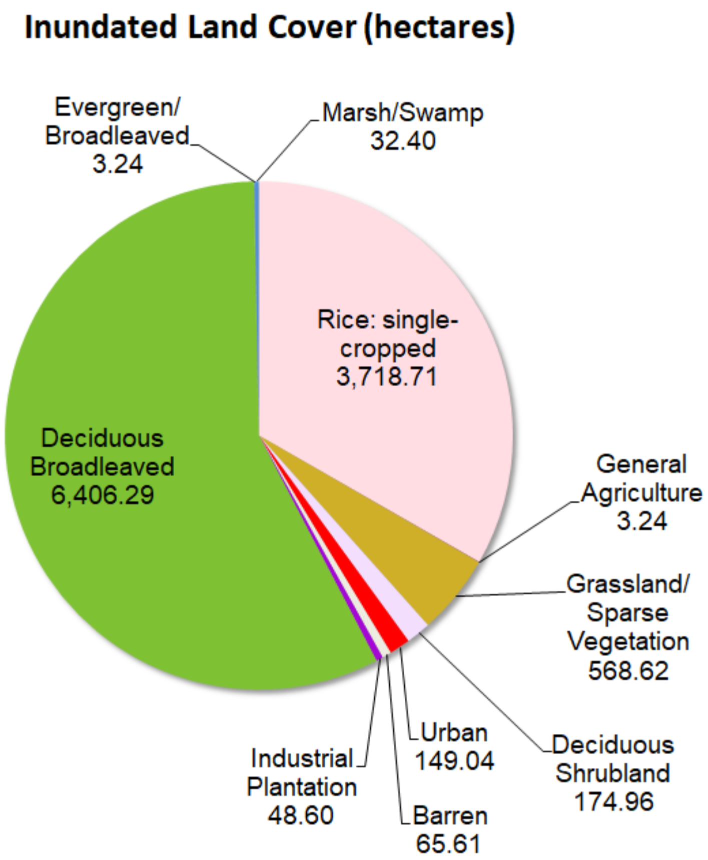

PI: John Bolten (NASA GSFC)
Project Scientists: Perry Oddo (NASA GSFC), Aakash Ahamed (Stanford U.)
Contributors: NASA SERVIR, NASA MSFC, SIG, ADPC

Flood Damage Assessment System Activated for July 25 Laos Dam Break

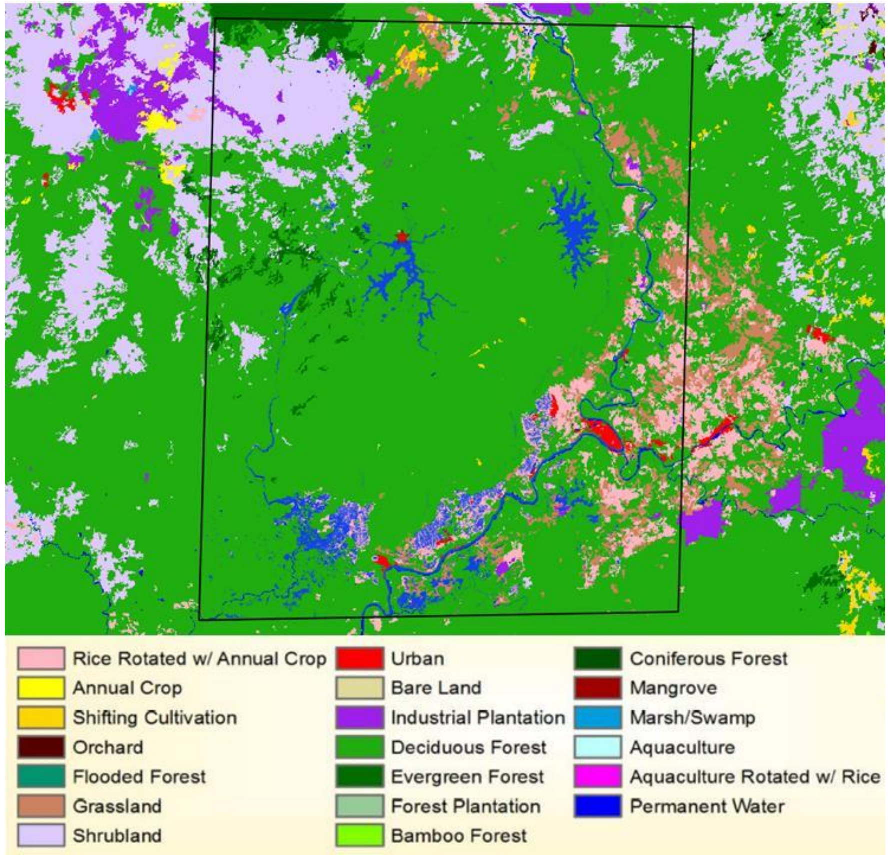

- Sentinel 1 and ALOS 2 data were used to derive flood inundation map for affected lands in Laos (leads: NASA SERVIR, NASA MSFC, SIG, U. of Houston, ADPC)
- Flood inundation depths estimated using Triangular Interpolated Network extracted from MERIT DEM elevations
- Socio-Economic data from OpenStreetMap and WorldPop used to estimate flood impact based on depth estimates
- Damage estimates calculated using estimated flood depths and Dutch ‘Standard Method’

PI: John Bolten (NASA GSFC)
Project Scientists: Perry Oddo (NASA GSFC), Aakash Ahamed (Stanford U.)
Contributors: NASA SERVIR, NASA MSFC, SIG, ADPC

Flood Damage Assessment System Activated for July 25 Laos Dam Break

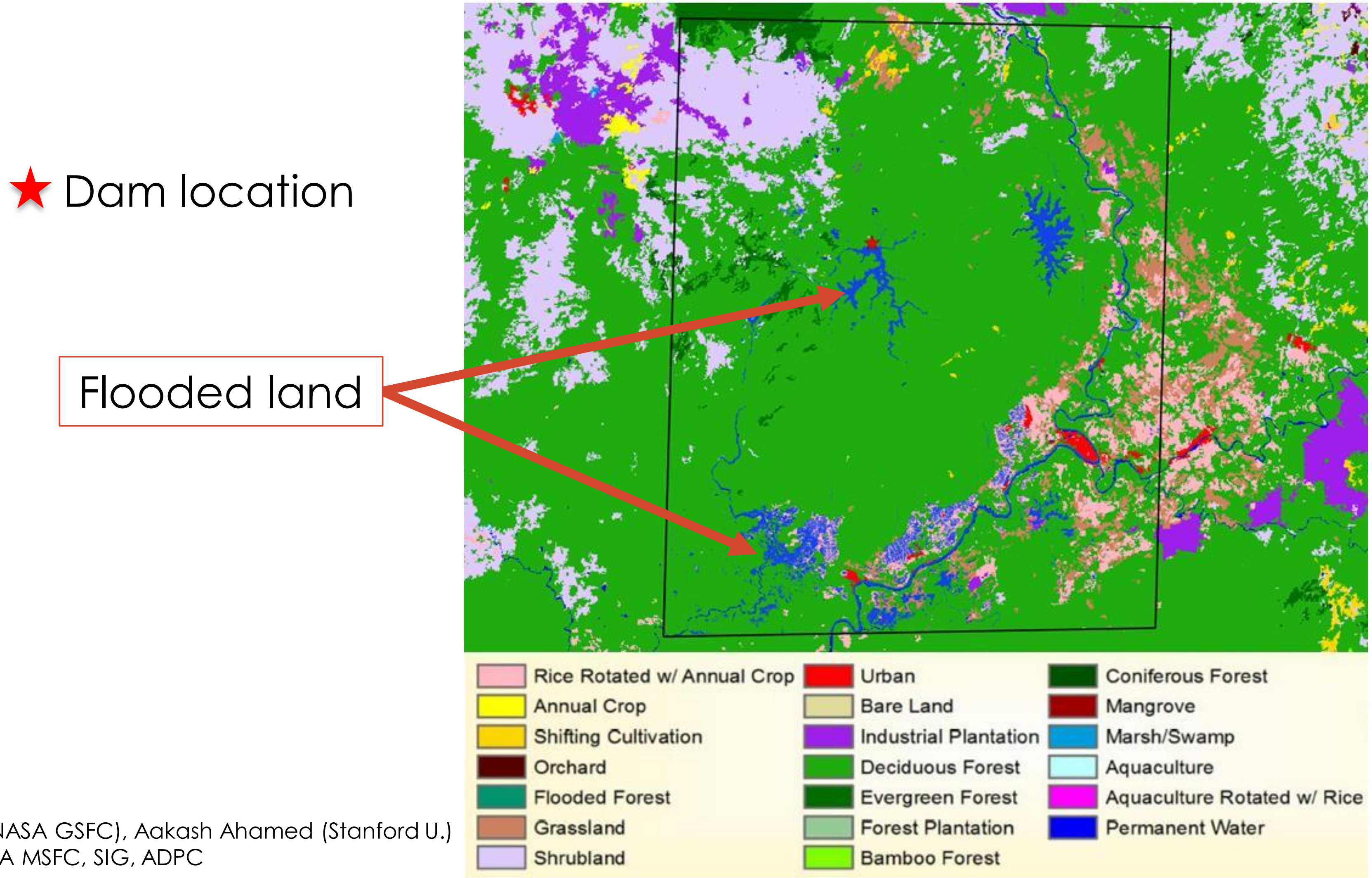

PI: John Bolten (NASA GSFC)
Project Scientists: Perry Oddo (NASA GSFC), Aakash Ahamed (Stanford U.)
Contributors: NASA SERVIR, NASA MSFC, SIG, ADPC

Value of NRT Earth Observations

VALUE IN HEALTH 17 (2014) 555–560

Available online at www.sciencedirect.com

ScienceDirect

journal homepage: www.elsevier.com/locate/jval

Time Is Money, But How Much? The Monetary Value of Response Time for Thai Ambulance Emergency Services

CrossMark

Henrik Jaldell, PhD[1,*], *Prachaksvich Lebnak, MD*[2], *Anurak Amornpetchsathaporn, MD*[2]

[1]*Department of Economics, Karlstad University, Karlstad, Sweden;* [2]*Emergency Medical Institute Thailand, Bangkok, Thailand*

ABSTRACT

Objective: To calculate the monetary value of the time factor per minute and per year for emergency services. **Methods:** The monetary values for ambulance emergency services were calculated for two different time factors, response time, which is the time from when a call is received by the emergency medical service call-taking center until the response team arrives at the emergency scene, and operational time, which includes the time to the hospital. The study was performed in two steps. First, marginal effects of reduced fatalities and injuries for a 1-minute change in the time factors were calculated. Second, the marginal effects and the monetary values were put together to find a value per minute. **Results:** The values were found to be 5.5 million Thai bath/min for fatality and 326,000 baht/min for severe injury. The total monetary value for a 1-minute improvement for each dispatch, summarized over 1 year, was 1.6 billion Thai baht using response time. **Conclusions:** The calculated values could be used in a cost-benefit analysis of an investment reducing the response time. The results from similar studies could for example be compared to the cost of moving an ambulance station or investing in a new alarm system.

Keywords: cost-benefit, emergency medical service, medicine, response time.

Value of NRT Earth Observations

VALUE IN HEALTH 17 (2014) 555–560

ELSEVIER

Available online at www.sciencedirect.com

ScienceDirect

journal homepage: www.elsevier.com/locate/jval

Time Is Money, But How Much? The Monetary Value of Response Time for Thai Ambulance Emergency Services

CrossMark

Henrik Jaldell, PhD[1,*], *Prachaksvich Lebnak, MD*[2], *Anurak Amornpetchsathaporn, MD*[2]

[1]*Department of Economics, Karlstad University, Karlstad, Sweden;* [2]*Emergency Medical Institute Thailand, Bangkok, Thailand*

ABSTRACT

Objective: To calculate the monetary value of the time factor per minute and per year for emergency services. **Methods:** The monetary values for ambulance emergency services were calculated for two different time factors, response time, which is the time from when a call is received by the emergency medical serv until the response team arrives at the emerger tional time, which includes the time to the ho: performed in two steps. First, marginal effects and injuries for a 1-minute change in the time fa Second, the marginal effects and the monet together to find a value per minute. **Results:** The values were found to be 5.5 million Thai bath/min for fatality and 326,000 baht/min for severe injury. The total monetary value for a 1-minute improvement for each dispatch, summarized over 1 year, was 1.6 billion Thai baht using response time. **Conclusions:** The calculated values could be used in a cost-benefit analysis of an investment reducing the response

The total monetary value for a 1-minute improvement for each dispatch, summarized over 1 year, was 1.6 billion Thai baht using response time.

Tethys App for Visualizing and Sharing Inputs/Outputs of the LMRB SWAT Model

http://tethys-servir.adpc.net/apps/swat2/

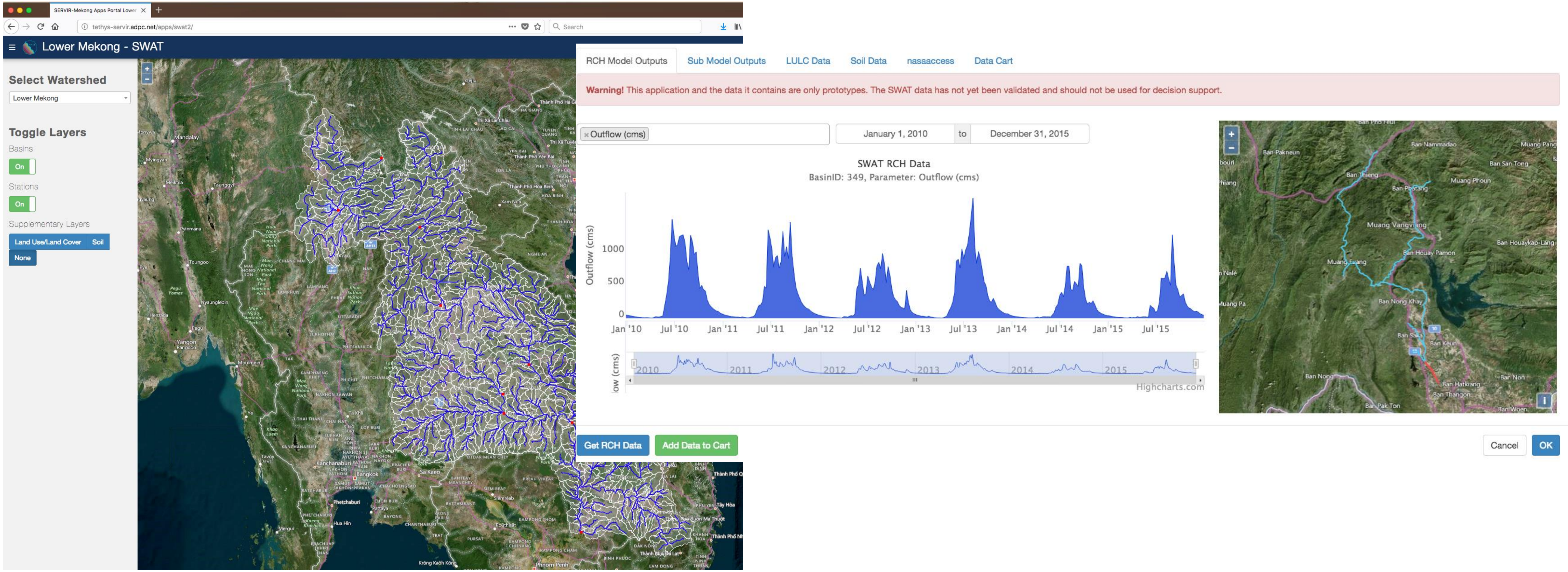

Mohammed, I.N., Bolten, J.D., Srinivasan, R., Lakshmi, V., 2018. Satellite observations and modeling to understand the Lower Mekong River Basin streamflow variability. J. Hydrol. 564, 559-573, https://doi.org/10.1016/j.jhydrol.2018.07.030

Tethys SWAT Tool

Data Sources

- **Elevation:** MERIT DEM (90 m)
- **Flood Extent**:
  - 2011 case study: ENVISAT-ASAR Wide Swath Mode (ESA)
  - NRT (future implementation): Will use flood detection output from Project Mekong (NASA LANCE MODIS-derived)
- **Land Cover**: Mekong River Commission
  - Landsat-based 30 m resolution, resampled to 90 m
- **Infrastructure**
  - Building footprints: OpenStreetMaps (accessed through Mapzen interface)
  - Roads: Global Roads Open Access Data Set (gROADS), v1 (NASA SEDAC)
- **Population**:
  - Gridded Population of the World (GPW), v4 (NASA SEDAC)


adpc
About Us
Publications
ADPC Ac
About Us
ADPC AT A GLANCE


ខ្មែរ | ລາວ | ภาษาไทย | Tiếng Việt | Webmail | Contact
Mekong River Commission
For Sustainable Development
Search MRC
GO
Home
About MRC
Mekong Basin
Topics
Publications
News & Events
Working with MRC
Highlights
Data Portal
MRC FAMILY TREE 2019
Key suggestions to manage risks for Pak Lay
Read the full story
From 11th to 18th March 2019, water levels along the lower Mekong River from Thailand's Chiang Saen to Lao PDR's Luang Prabang were fluctuated above their long-term averages (LTAs) the same trend as last week, although no rainfall in these areas. The trend from 19th to 25th March 2019 will be gradually slightly increasing and still keep stays above their LTAs. For downstream reaches from Lao PDR's Vientiane to Cambodia's Kompong Cham, the trends will be the same as upstream part. The lower reaches from Cambodia's Phnom Penh at Chaktomuk, koh Khel, Neak Luong to Viet Nam's Tan Chau on the Mekong River and Chau Doc on the Bassac River will be slightly increasing and stay above their LTAs due to the abnormal rainfall in March 2019 in the floodplain area.
Forecasted water level for 22 stations (updated every Monday) more »
Observed water level compared to long term average for 13 stations (updated every Monday) more »

Applied Remote Sensing for Improved Transboundary Water Resource Management

Lower Mekong River Basin

John D. Bolten[1], I. Mohammed[1], and J. Spruce[2], P. Oddo[1], V. Lakshmi[3], C. L. Hung[3], R. Srinivasan[4], C. Doyle[1], D. Nguyen[5], Nelson[6], S. McDonald[6], C. MeeChaiya[7], P.Towashiraporn[7], S. Pulla[8], A. (Weigel) Markert[8]

[1]NASA Goddard Space Flight Center

[2]*NASA Stennis Space Center*

[3]*University of South Carolina*

[4]*Texas A&M University*

[5]*Mekong River Commission*

[6]*Brigham Young University*

[7]*Asian Disaster Preparedness Center, Bangkok, Thailand*

[8]*NASA Marshall Spaceflight Center*

References

- Oddo, P., A. Ahamed, and J. Bolten. 2018. "Socioeconomic Impact Evaluation for Near Real-Time Flood Detection in the Lower Mekong River Basin." Hydrology, 5 (2): 23 [10.3390/hydrology5020023]
- Mohammed, I., J. Bolten, R. Srinivasan, and V. Lakshmi. 2018. "Improved Hydrological Decision Support System for the Lower Mekong River Basin Using Satellite-Based Earth Observations." Remote Sensing, 10 (6): 885 [10.3390/rs10060885]
- Mohammed, I. N., J. D. Bolten, R. Srinivasan, and V. Lakshmi. 2018. "Satellite observations and modeling to understand the Lower Mekong River Basin streamflow variability." Journal of Hydrology, 564: 559-573 [10.1016/j.jhydrol.2018.07.030]
- Le, H., J. Sutton, D. Bui, J. Bolten, and V. Lakshmi. 2018. "Comparison and Bias Correction of TMPA Precipitation Products over the Lower Part of Red–Thai Binh River Basin of Vietnam." Remote Sensing, 10 (10): 1582 [10.3390/rs10101582]
- Mohammed, I. N., J. D. Bolten, R. Srinivasan, et al. 2018. "Ground and satellite based observation datasets for the Lower Mekong River Basin." Data in Brief, 21: 2020-2027 [10.1016/j.dib.2018.11.038]
- Spruce, J., J. Bolten, R. Srinivasan, and V. Lakshmi. 2018. "Developing Land Use Land Cover Maps for the Lower Mekong Basin to Aid Hydrologic Modeling and Basin Planning." Remote Sensing, 10 (12): 1910 [10.3390/rs10121910]
- Fayne, J. V., J. D. Bolten, C. S. Doyle, et al. 2017. "Flood mapping in the lower Mekong River Basin using daily MODIS observations." International Journal of Remote Sensing, 38 (6): 1737-1757 [10.1080/01431161.2017.1285503]
- Ahamed, A., and J. Bolten. 2017. "A MODIS-based automated flood monitoring system for southeast asia." International Journal of Applied Earth Observation and Geoinformation, 61: 104-117 [10.1016/j.jag.2017.05.006]
- Ahamed, A., J. D. Bolten, C. Doyle, and J. Fayne. 2016. "Near Real-Time Flood Monitoring and Impact Systems." Remote Sensing of Hydrological Extremes, 105-118 [10.1007/978-3-319-43744-6]

References

- Fayne, J., J. Bolten, V. Lakshmi, and A. Ahamed. 2016. "Optical and Physical Methods for Mapping Flooding with Satellite Imagery."Remote Sensing of Hydrological Extremes, 83-103 [10.1007/978-3-319-43744-6_5]
- Bolten, J., and W. Crow. 2012. "Improved prediction of quasi-global vegetation conditions using remotely-sensed surface soil moisture." Geophysical Research Letters, 39 (19): L19406 [10.1029/2012GL053470]
- Nicholls, R. J. et al. Ranking Port Cities with High Exposure and Vulnerability to Climate Extremes. (Organisation for Economic Co-operation and Development, 2008).
- 2018. "Global Hydrological Cycles and Water Resources." National Academies of Sciences, Engineering, and Medicine. 2018. Thriving on Our Changing Planet: A Decadal Strategy for Earth Observation from Space, Washington, DC: The National Academies Press [10.17226/24938]
- Rossi, et. al., 2009. Hydrologic evaluation of the lower Mekong River Basin with the soil and water assessment tool model. IAEJ 18, 1-13, http://114.255.9.31/iaej/EN/Y2009/V18/I01-02/1
- Gassman, P.W., Reyes, M.R., Green, C.H., Arnold, J.G., 2007. The soil and water assessment tool: Historical development, applications, and future research directions. T ASABE 50, 1211-1250, https://doi.org/10.13031/2013.23637
- Cham, T. C., Mitani, Y., Fujii, K. & Ikemi, H. Evaluation of flood volume and inundation depth by GIS midstream of Chao Phraya River Basin, Thailand. in WIT Transactions on The Built Environment (ed. Brebbia, C. A.) 1, 1049–1060 (WIT Press, 2015).
- Kok, M., Huizinga, H. J., Vrouwenfelder, A. & Barendregt, A. Standard method 2004. Damage and casualties caused by flooding. (Rijkswaterstaat, 2004).